Multiple Wave Approximation Algorithm for Solving Hyperbolic Partial Differential Equations

Sian Huey Tong

A thesis presented for the degree of

Master of Science in Computational Engineering

Universitetet
i Stavanger

Abstract

In this thesis, we present a new perspective on the *large time step wave adding scheme* and *two/three wave approximation* from the papers by Dong [1] and Qian [9] respectively. Subsequently, this thesis intends to provide a unified framework such that LTS-Roe, LTS-Godunov, and wave adding scheme and wave approximation method are significantly related. By elaborating the concept of waves approximation into one-wave, it is essentially LTS-Roe describing the wave interaction as a linearised function. Furthermore, a two-waves and a three-waves are approximations by increasing into two and three linearised functions respectively. Instead, for LTS-Godunov describes the wave interaction in its original flux function and is interpreted as the *'quadratic'* flux of LTS-WA.

We also provide a revision of the aforementioned schemes by improving the logic flow of the schemes by introducing LTS schemes and wave approximation algorithms for a more extensive application in hyperbolic conservation laws. The reformulation of the waves approximation is relabelled as 'two-N-waves approximation' and 'three-N-waves approximation'. In addition to revising the schemes, we take into account of solving non-convex function with LTS schemes and wave approximations as opposed to solely concave or convex functions. Thereby, establishing an interest in investigation, particularly in Buckley-Leverett (BL) flux function, the study of the equation entails. While performing computational calculation for extrema function of LTS scheme with BL function, we then introduce an analytical solution to reduce the computation time. However, the analytical solution only limits to constant $M = 1$, thus present a new problem.

To validate the frameworks, numerical simulations are performed beginning with LTS scheme: Godunov scheme. Then, an analysis of the LTS-Roe in rarefaction wave, followed by transonic rarefaction and system of equations. Thereafter, several tests from Dong's paper [1] are reproduced of which are implementing LTS-Roe, LTS-Godunov, and the reformulated three-N-waves-approximation in comparison with Dong's LTS-WA and wave-approximation. The results are validated with identical plots as the paper. Finally, the test for BL is assessed with different choices of courant number and grid cells which result in a great resolution at high courant number specifically 13.1 in this thesis when compared to the exact solution, therefore proving the robustness and accuracy of the algorithms and solutions provided for non-convex function.

Acknowledgements

I would like to express my many thanks to my supervisor, Tore Halsne Flåtten. Without his guidance and support, I will not be able to complete this thesis.

Contents

List of Figures

List of Tables

Chapter 1

Introduction

Numerical methods of hyperbolic conservation laws are constricted by CFL stability condition where the domain of dependence of the numerical solution must be within the analytical solution's domain of dependence. The CFL number is traditionally restricted to be less than 1 due to the hyperbolicity, however, the development of large time step (LTS) schemes allows CFL to be greater than 1. Thereby the CFL condition is extended from CFL= $f'(u)\frac{\Delta t}{\Delta x} \leq 1$ to CFL$\leq k$, where k is the number of computational neighbouring cells. With that, the conserved quantity is allowed to convect to arbitrary k cells away. The grid cell stencils are then extended from the traditional three points to $(2k+1)$ cells.

We are investigating large time step (LTS) explicit schemes that uses an exact or approximate Riemann solver and wave adding method, proposed by LeVeque [4] and multiple wave approximation by Qian [9]. The developed LTS-Godunov scheme tracks the spreading of every rarefaction wave throughout k computational cells. LeVeque proposed three ways to handle the rarefaction wave addition: first is to integrate the rarefaction fan, second is to replace the rarefaction fan with a series of discontinuities such that enough discontinuities lead to a better approximation, third is to simply linearise the original conservation laws locally thus solving Riemann problem and wave adding to yield final solutions of the scheme. Whereas Qian proposed the multiple wave approximation which is an umbrella term for two-wave approximation and three-waves approximation. It is to inhibit rarefaction shocks from occurring when performing numerical computations. Every rarefaction discontinuity wave satisfies the Rankine-Hugoniot condition. The rarefaction discontinuity waves are linearly interpolated for any Riemann problem or in other words any discontinuity of the original rarefaction wave. Theoretically, it can extend to more than just two or three waves, however it comes with the cost of computation expense, thus three waves is sufficient to approximate most of the functions in this present study.

The state of the aforementioned schemes introduced have concepts that are distant from each other, however that is not the case. Thus, in this thesis we intend to clear the air of these concepts therefore provide a unifying framework in particularly LTS-Roe, LTS-Godunov, wave adding scheme and multi-wave approximation.

1.1 Organisation of Thesis

The thesis is allocated into five chapters, each chapter assesses components and approach to provide perspective for unifying LTS, wave addition and wave approximation framework.

Chapter 1 (Introduction) presents the preface of the schemes that were established in the past. Hereby we provide a preliminary explanation of the LTS schemes and the thesis's objective.

Chapter 2 (Background) explicates the mathematical models and numerical methods that are essential for the hyperbolic conservation law and extension to LTS schemes.

Chapter 3 (N-Waves Approximation) describes the methodical approach in revising the wave approximation method by Dong. In an overview, we propose N-waves algorithms that are named 'two-N-waves approximation' and 'three-N-waves approximation'. Moreover, we discuss the properties of non-convex equations particularly the Buckley-Leverett equation for further investigation towards LTS schemes and the newly revised N-waves approximation.

Chapter 4 (Numerical Simulation) delivers the numerical simulation and results of Godunov and LTS-Roe in the one-dimensional Burgers equation. We also present the simulations of LTS-Roe for the 2x2 shallow water system by implementing LTS-Roe. Then, three tests are of results that are of reproduction of the tests in Dong's paper, of which are compared with LTS-Roe, LTS-Godunov, and the reformulated N-waves approximation. Finally, we present the simulation of the Buckley-Leverett equation as well as the approach in obtaining a more efficient computation analytically.

Chapter 5 (Conclusion) delivers definitive remarks of all the results obtained in this research and summarise the relationship among the schemes presented. Lastly, we suggest recommendations for further study on an area where the scope of study in Buckley-Leverett function has not been achieved.

Chapter 2

Background

In this chapter, we discuss the mathematical models and numerical methods. The fundamental concepts of scalar conservation law and the properties of the solution are introduced in particular of solution uniqueness and its entropy condition. *Godunov's method* serves as the starting point for methods towards linear and nonlinear hyperbolic systems. Lastly, we extend to large time step scheme in accordance with Lindqvist [6] and reference from Prebeg [8].

2.1 Conservation Law

The interactions of particles at macroscopic level is governed by fundamental principles of mechanics where the state of any particular physical properties or otherwise measurable quantities remain constant with respect to change of time in an isolated and closed system. Such law is known as *conservation law*. This phenomenon can be described as the rate of change of a quantity in any domain will be equal to the *flux*, representing the amount of quantity that enter and exits the surface of domain, and *source or sink*, expressed as the quantities that are created or destroyed respectively. It can be expressed mathematically as,

$$\frac{\partial}{\partial t}\int_{\Omega} \mathbf{U}\, dV = \underbrace{-\int_{\partial\Omega} \mathbf{F}\cdot\nu\, ds}_{\text{flux}} + \underbrace{\int_{\Omega} \mathbf{S}\, dV}_{\text{source}} \tag{2.1}$$

where vector $\mathbf{U}$ is the quantity of interest that may be mass or velocity of fluid or concentration of chemical through domain Ω. $\mathbf{F}$, vector field or simply think of it as fluid velocity passes through in the direction of ν, unit normal vector over the surface. $\mathbf{S}$ is the source through domain Ω.

The conservation law can be rewritten in differential form by integration by parts or Gauss divergence theorem, (2.1) becomes,

$$\frac{\partial \mathbf{U}}{\partial t} + \nabla\cdot\mathbf{F} = \mathbf{S} \tag{2.2}$$

Commonly, the only change of quantity of interest comes from the flux, thus the source is set to be zero. Also for simplicity, the differential form reduces to one-dimensional space. Thus (2.2) simplifies to a general form of scalar conservation law, where u is the scalar of $\mathbf{U}$.

$$\frac{\partial u}{\partial t} + \frac{\partial}{\partial x} f(u) = 0 \tag{2.3}$$

2.2 Scalar Conservation Laws

The general form of scalar conservation law with its initial condition can be presented as:

$$u_t + f(u)_x = 0 \tag{2.4a}$$
$$u(x, 0) = u_0(x) \tag{2.4b}$$

where $u(x, t)$ is the unknown and the given functions being $f(u)$, a nonlinear function and $u_0(x)$.

The solution of the initial value problem can be obtained with *method of characteristics*. Given a curve $(x(t), t)$ along the constant solution $u(x(t), t)$, means that

$$\frac{d}{dt} u(x(t), t) = 0$$
$$u_x(x(t), t) \cdot x'(t) + u_t(x(t), t)) = 0$$

therefore, it follows that u is constant along $(x(t), t)$. A solution exists such that

$$x'(t) = f'(u_0(x_0)) \tag{2.5a}$$
$$x(t = 0) = x_0 \tag{2.5b}$$

provided that $f'(u_0(x_0))$ is Lipschitz continuous in (2.5). It is then solved explicitly as $x(t) = x_0 + f'(u_0(x_0))t$, also known as the characteristic equation. The unique solution for $u(x, t)$ is thus

$$u(x, t) = u_0\big(x - f'(u_0(x_0))t\big) \tag{2.6}$$

Despite smooth initial data, any nonlinear function f may still subject to characteristics curve intersection. Such phenomenon occurs when the left wave $f'(u_l)$ is higher than the right wave $f'(u_r)$ that leads to a *shock* which is a discontinuous solution. A continuous solution for any left and right states will otherwise result in a continuous solution, which is a *rarefaction*. The interest towards the problem lies in the discontinuities, when a shock is present, the function is not differentiable. To allow a discontinuous solution, a *weak solution* is introduced, in the sense that a *compact support* where a finite domain allows continuously differentiable functions and 0 outside of the domain. This problem is then boiled down to a Riemann problem.

2.2.1 Riemann Problem

A Riemann problem is an initial value problem for hyperbolic conservation laws with piecewise constant initial data such that two constant states are separated by a discontinuity.

$$u(x, 0) = \begin{cases} u_L & , x < 0 \\ u_R & , x > 0 \end{cases} \tag{2.7}$$

the expression is a generalisation of a Riemann problem. Two kinds of solutions are to construct to bridge this discontinuity. First being the continuous solution or *rar-*

efaction solution and the second being the discontinuous solution or *shock solution*. The following formulation is described for cases with convex function $f''(u) > 0$.

Rarefaction solution:

$$u(x,t) = \begin{cases} u_L & , \frac{x}{t} \leq f'(u_L) \\ (f')^{-1}(\frac{x}{t}) & , f'(u_L) \leq \frac{x}{t} \leq f'(u_R) \\ u_R & , f'(u_R) \leq \frac{x}{t} \end{cases} \tag{2.8}$$

Shock solution:

$$u(x,t) = \begin{cases} u_L & , x \leq st \\ u_R & , x \leq st \end{cases} \tag{2.9}$$

where s is the shock speed and defined by the Rankine-Hugoniot condition:

$$s = \frac{f(u_R) - f(u_L)}{u_R - u_L} \tag{2.10}$$

Shock solution is an approach for a type of weak solution, which allows convenience to obtain bounded solution, however, it is not a strict solution. In reality, when approaching a shock wave, viscous terms are essential as they describe a smooth transition over a thin region instead of a sharp discontinuity. For instance, effects of viscosity in gas molecules or the motions when gases are mixed with a concentration gradient. The viscosity term, ϵ can be seen as an additional term in the conservation equation

$$u_t + f(u)_x = \epsilon q_{xx} \tag{2.11}$$

As ϵ approaches zero, the equation will return to the form (2.4a). The motivation of introducing the viscous term is to have a realisation for *hyperbolic conservation law* whereby the viscous term is neglected. The idea of vanishing viscosity by looking at the limit $\epsilon \to 0$ is to define a rational solution for a hyperbolic equation which will be discussed in the later section. In numerical schemes, it is extremely useful for simplicity and is able to model closely how the exact solution will behave near shock wave.

2.2.2 Entropy Condition

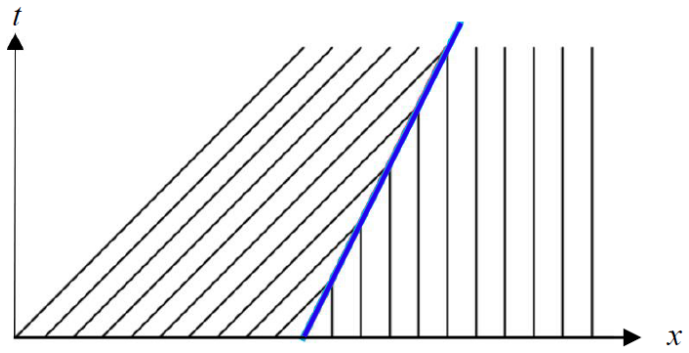

Figure 2.1: Characteristic solution by solving $x(t) = x_0 + f'(u_0(x_0))t$ for shock. It shows that the characteristics slowly converge into a meeting point also referred to as the breaking time. Solution after breaking time is determined along the coloured line.

Having said that shock solution is a valid weak solution to the Riemann problem. A decreasing jump or a decreasing discontinuity such that the u_L, left wave speed is higher than u_R, right wave speed, it is then said to have a discontinuity known as shock. An illustration of this shock solution is seen in Figure 2.1. The discontinuity propagates with s, speed described by Rankine-Hugoniot condition in equation 2.10 and satisfies the *Lax entropy condition* when

$$f'(u_L) > s > f'(u_R) \tag{2.12}$$

This condition strictly applies on a convex flux function in which $u_L > u_R$, then $f'(u_L) > f'(u_R)$.

Conversely, the Lax entropy condition is not satisfied when there is an increasing initial jump. An increasing discontinuity such that u_L is lower than u_R, a rarefaction wave. The rarefaction solution is illustrated in Figure 2.2. Despite $u_L < u_R$, then $f'(u_L) < f'(u_R)$ not satisfying Lax entropy condition, rarefaction solution (2.9) still exists and applicable as a weak solution.

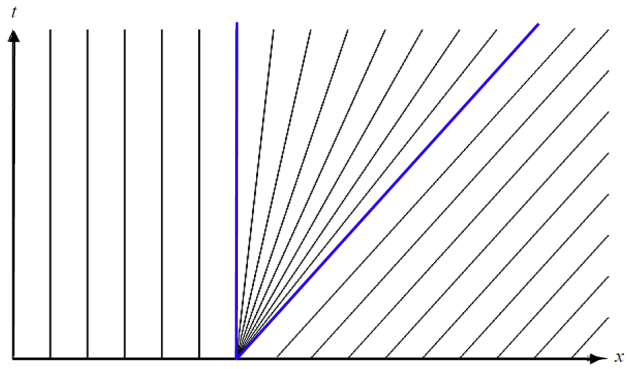

Figure 2.2: Characteristic solution by solving $x(t) = x_0 + f'(u_0(x_0))t$ for rarefaction. The characteristics slowly expand from a discontinuity forming an expansion fan a region indicated between two coloured lines.

2.3 Hyperbolic Conservation Laws

The focus of this thesis revolves around coupling advective transport and wave flow or simply hydrodynamics. With that lies the basis of solving hyperbolic systems, meaning solving first order systems of partial differential equations. Considering a hyperbolic system of conservation law:

$$\frac{\partial \mathbf{U}}{\partial t} + \frac{\partial}{\partial x}\mathbf{f}(\mathbf{U}) = 0 \tag{2.13}$$

$$u(x, 0) = u_0(x) \tag{2.14}$$

where $\mathbf{U} \in \mathbb{R}^N$ and $\mathbf{f} : \mathbb{R}^N \to \mathbb{R}^N$. The conserved variables and flux function are of vectors and with chain rule it can be rewritten in a closed form expression:

$$\frac{\partial u_i}{\partial t} + \sum_{j=1}^{N} \frac{\partial f_i}{\partial u_j}\frac{\partial u_j}{\partial x} = 0 \tag{2.15}$$

and the system of equations can be in a quasilinear form with its matrix form

$$\frac{\partial \mathbf{U}}{\partial t} + \mathbf{A}(\mathbf{u})\frac{\partial \mathbf{U}}{\partial x} = 0 \tag{2.16}$$

where matrix ***A(u)*** is the $N \times N$ Jacobian matrix of the flux vectors. The hyperbolicity of the system is denoted by the diagonalizability of Jacobian matrix and its resulting eigenvalues are *real*.

2.3.1 Characteristic Decomposition

With a complete set of eigenvectors, there exist corresponding eigenvalues such that:

$$AR = \Omega R \tag{2.17}$$

By defining a matrix of eigenvectors, R and diagonal matrix of eigenvalues, Ω. The underlying matrix A can be defined as

$$A = R\Omega R^{-1} \tag{2.18}$$

Considering a vector of characteristics variables

$$d\mathbf{C} = R^{-1}d\mathbf{U} \tag{2.19}$$

The diagonalisation of ***A(u)*** together with a vector of characteristic variables, $\mathbf{A}(\mathbf{u})$ allows the (2.16) quasilinear conservation law form to decompose simply by multiplying inverse eigenvectors of the Jacobian matrix:

$$\begin{aligned} R^{-1}\frac{\partial \mathbf{U}}{\partial t} + R^{-1}\mathbf{A}(\mathbf{u})\frac{\partial \mathbf{U}}{\partial x} &= 0 \\ R^{-1}\frac{\partial \mathbf{U}}{\partial t} + R^{-1}R\Omega R^{-1}\frac{\partial \mathbf{U}}{\partial x} &= 0 \\ \frac{\partial \mathbf{C}}{\partial t} + R^{-1}R\Omega\frac{\partial \mathbf{C}}{\partial x} &= 0 \\ \frac{\partial \mathbf{C}}{\partial t} + \Omega\frac{\partial \mathbf{C}}{\partial x} &= 0 \end{aligned}$$

The hyperbolic system can be rewritten in the form of components:

$$\mathbf{C}_t^i + \lambda^i \mathbf{C}_x^i = 0 \tag{2.20}$$

where C^i is the i-th component of $C(x,t)$ and its corresponding eigenvalue λ^i. With that this decoupled transport equation can be solved with the method of characteristic.

2.4 Finite Volume Method

The finite volume method is a method for representing and evaluating partial differential equations. The equations are discretized into a finite number of control volumes, in which the volume integrals are reformed in surface integrals with Gauss divergence theorem as was discussed in section 2.1.

2.4.1 Grid Cells

Consider a uniform discretization of a one-dimensional *space* domain with boundaries [x_L,x_R], where $\Delta x = \frac{x_L - x_R}{N}$. Δx can be defined as the computational grids or

control volumes,

$$CV_j = [x_{j-1/2}, x_{j+1/2}] \tag{2.21}$$

the number of such grids are determined by N. *Time* is also discretized uniformly into equal size Δt, so that the time levels are denoted by

$$t^n = n\Delta t \tag{2.22}$$

2.4.2 Cell average

The dependent values of finite volume method are stored in the centre of the control volumes. Unlike finite difference, which is stored at the nodes, FVM ensures conservation of mass, momentum, and energy at each cell grids. Therefore, the conservation law is integrated over the control volume, hence cell averages. At each time step, we solve for an approximation of the exact cell average of exact solution.

$$u_i^n \approx \frac{1}{\Delta x} \int_{x_{j-1/2}}^{x_{j+1/2}} u(x, t^n) dx \tag{2.23}$$

2.4.3 Numerical Flux

To approximate the exact total flux between two neighbouring cells in a time step at the interface $x_{j+1/2}$,

$$F_{j+1/2}^n \approx \frac{1}{\Delta t} \int_{t^n}^{t^{n+1}} f(u(x_{j+1/2}, t)) dt \tag{2.24}$$

more of the numerical flux will be discussed in detail, whereby there are many developed methods of the approximations of the exact flux.

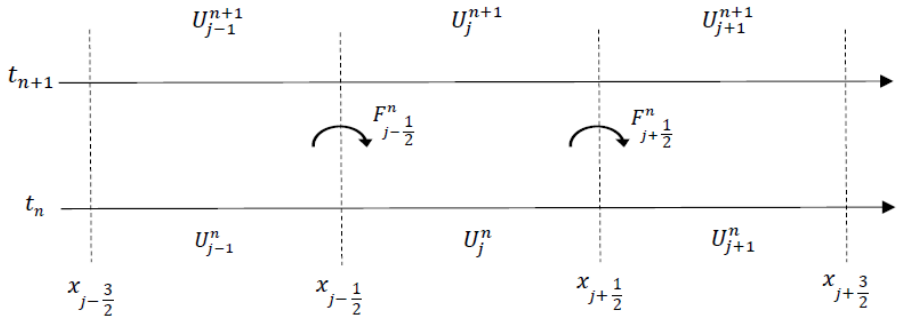

Figure 2.3: Finite volume grid cells spatial and temporal discretization

2.4.4 General Formulation

We wish to approximate the target quantity after a time step of length Δt — U_j^{n+1}. By integrating the conservation law over space-time continuum $[x_{j-1/2}, x_{j+1/2}) \times [t^n, t^{n+1})$:

$$\int_{t^n}^{t^{n+1}} \int_{x_{j-1/2}}^{x_{j+1/2}} U_t dx dt + \int_{t^n}^{t^{n+1}} \int_{x_{j-1/2}}^{x_{j+1/2}} f(U)_x dx dt = 0 \tag{2.25}$$

then with fundamental theorem of calculus, gives

$$\int_{x_{j-1/2}}^{x_{j+1/2}} U(x,t^{n+1})dx - \int_{x_{j-1/2}}^{x_{j+1/2}} U(x,t^{n})dx + \int_{t^n}^{t^{n+1}} f(U(x_{j+1/2,t}))dt - \int_{t^n}^{t^{n+1}} f(U(x_{j-1/2,t}))dt = 0 \quad (2.26)$$

incorporating with the defined equations (2.23) and (2.24), then divide (2.25) by Δx, the form is then reduced to:

$$U_i^{n+1} = U_i^n - \frac{\Delta t}{\Delta x}(F_{j+1/2}^n - F_{j-1/2}^n) \quad (2.27)$$

this form of numerical method is known as the conservative scheme. It is conservative because all the terms are inclusive such that the flux is not approximated and all quantities are still preserved. In general for an explicit method with *three point scheme* in one dimensional space where U_j^{n+1} is dependent on three points/values U_{j-i}^n U_i^n, and U_j^n. This dependence leads to a formulation that includes a numerical viscosity coefficient $Q_{j+1/2}^n$, thereby the general numerical flux formulation is given as,

$$F_{j+1/2}^n = \frac{1}{2}(f(U_j^n) + f(U_{j+1}^n)) - \frac{1}{2}\frac{\Delta x}{\Delta t}Q_{j+1/2}^n(U_{j+1}^n - U_j^n) \quad (2.28)$$

then by simply computing the difference of the fluxes $F_{j+1/2}^n$ and $F_{j-1/2}^n$, equation (2.27) is then rewritten in this general form:

$$U_i^{n+1} = U_i^n - \frac{\Delta t}{\Delta x}\big(A_{j-1/2}^+(U_j^n - U_{j-1}^n) + A_{j+1/2}^-(U_{j+1}^n - U_j^n)\big) \quad (2.29)$$

A approximates the derivative of the flux function, where $A = A_{j-1/2}^+ + A_{j+1/2}^-$, if otherwise a flux function is linear, then A is simply a constant. All in all, it is essentially an approximation of the nonlinear equation by *linearizing* it. The approximation of the flux function is represented by

$$\begin{aligned} f(U)_x &= f'(U) \cdot U_x \\ &\approx \hat{A}_{j+1/2}U_x \end{aligned}$$

There are many existing developed methods to tackle the approximation of flux numerically, some has advantages over the other, which also motivates the formulation of alternative numerical fluxes.

2.4.5 CFL Condition

A one-dimensional advection equation such like formulated in 2.27 requires that CFL condition to achieve stability by

$$CFL = f'(u)\frac{\Delta t}{\Delta x} \leq 1 \quad (2.30)$$

where $f'(u)$ is the derivative of the flux function. The resulting non-dimensional number is referred to as the *courant number*. In any case, the stability of an explicitly defined conservative scheme must traditionally require CFL condition to be bounded.

2.4.6 Numerical Diffusion

The CFL condition is necessary for the scheme to be stable, however, it does not provide any basis for accuracy for a *three point scheme*. Basing on equation (2.28), the term numerical viscosity coefficient, Q, can be regarded as an estimate in discretised equation that approximates the advection equation.

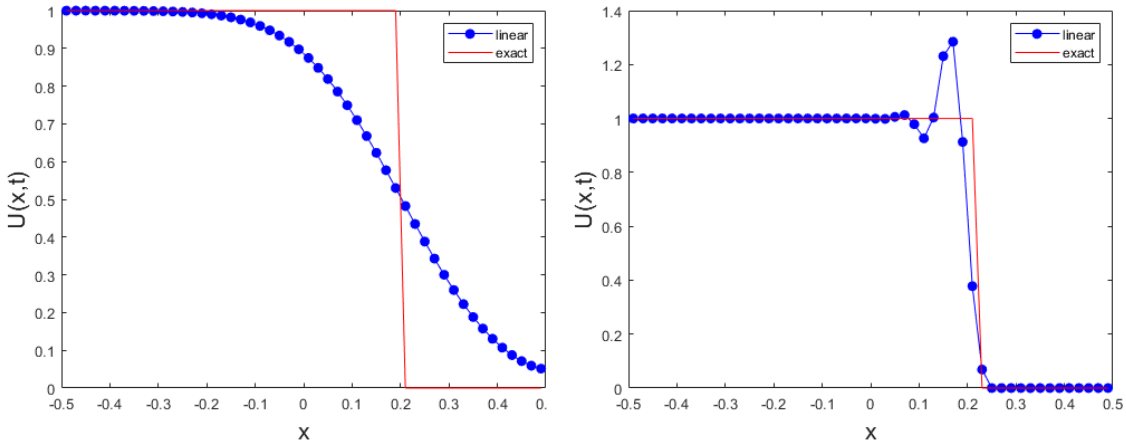

(a) *Courant = 0.1* (b) *Courant = 0.9*

Figure 2.4: Advection scheme with $Q = 0.7$. It shows that a large Q to Courant ratio provides stability for the cost of large diffusion, conversely a small Q to Courant ratio renders accuracy for the cost of instability.

The error that arises when discretised is the truncation error, that is through negating higher order Taylor expansion. This error is dependent on the diffusion term, thus when CFL tends to 1, the error vanishes and solve exactly. The trade-off is where the diffusion term dampens the instabilities for a large courant number, resulting in more diffusion and smearing effect.

2.4.7 Flux Difference and Numerical Viscosity Coefficients

In relation to the general numerical flux formulation equation (2.28), there are different existing formulations of numerical fluxes by simply modifying the numerical viscosity, $Q_{j+1/2}$, or its equivalent in another form with flux difference coefficients, $A^{\pm}$ for flux difference equation 2.29. A summary of the established methods is shown in table 2.1.

Table 2.1: Numerical viscosity and flux difference coefficients

Scheme	$\boldsymbol{Q_{j+1/2}}$	$\boldsymbol{A^{\pm}}$
Roe	$a_{j+1/2}$	$\pm max(0, \pm a_{j+1/2})$
Lax-Friedrichs	1	$\frac{1}{2}(a_{j+1/2} \pm \frac{\Delta x}{\Delta t})$
Lax-Wendroff	$\left(f'(u)\frac{\Delta t}{\Delta x}\right)^2$ *or* $(C_{j+1/2})^2$	$\frac{1}{2}a_{j+1/2}\left(1 \pm a_{j+1/2}\frac{\Delta t}{\Delta x}\right)$
Godunov	$\frac{f_j + f_{j+1} - 2M_{j+1/2}(w(u))}{u_{j+1} - u_j}$	$\frac{1}{2}a_{j+1/2}\left(a_{j+1/2} \pm \frac{f_j + f_{j+1} - 2M_{j+1/2}(w(u))}{u_{j+1} - u_j}\right)$

where $a_{j+1/2}$ is $f'(u_j)$ or the Rankine-Hugoniot speed at cell j as described in 2.10, and $M_{j+1/2}\big(w(u)\big)$ is defined as,

$$M_{j+1/2}\big(w(u)\big) = \begin{cases} \min\limits_{u\in R_{j+1/2}} w(u) & u_j < u_{j+1} \\ \max\limits_{u\in R_{j+1/2}} w(u) & u_j \geq u_{j+1} \end{cases} \tag{2.31}$$

with $R_{j+1/2}$ defined as:

$$R = [\mathbf{min}(u_j, u_{j+1}), \mathbf{max}(u_j, u_{j+1})]$$

2.4.8 Total Variation Diminishing (TVD)

TVD is a property that ensures no oscillation occurs in numerical solution, which is also a verification for the nonlinear stability of numerical solution. TVD attempts to prevent the solution to overshoot at discontinuities that cause oscillation. The total variation of solution over the defined finite space is defined by

$$TV(u) = \int_{-\infty}^{\infty} |\frac{\partial u}{\partial x}| dx \tag{2.32}$$

where the scheme for a single time step can be rewritten in discrete form

$$TV(u^n) = \sum_{j=-\infty}^{\infty} |u_{j+1}^n - u_j^n| \tag{2.33}$$

The numerical scheme is said to be total variation diminishing when

$$TV(u^{n+1}) \leq TV(u^n) \tag{2.34}$$

For a 3-point scheme flux formulation discussed 2.28, the scheme will be unconditionally TVD if and only the numerical viscosity is

$$|a_{j+1/2}| \leq Q_{j+1/2} \leq 1$$
$$Q_{Roe} \leq Q_{j+1/2} \leq Q_{Lax-Friedrichs}$$

Otherwise, a general form of stability equation for a fully discrete equation (2.29) may be formulated as:

$$\frac{\Delta t}{\Delta x}(A_{j-1/2}^{+} + A_{j-1/2}^{-}) \leq 1 \tag{2.35}$$

2.5 Large Time Step Methods

To enable the CFL condition having more than 1 for the standard explicit conservative scheme (2.27), the large time step (LTS) method is employed to allow waves to travel more than one grid cell at a time step. Thereby, considering the original 3-point scheme ($2k$+1), which is conventionally $k = 0$, that is two ghost cells at each end. By extending the dependencies of the number of grid cells, we introduce local multipoint schemes which are discussed in the paper by Lindqvist [6]. This dependency is modified on its numerical flux function including more points in one-dimensional space where,

$$F_{j+1/2} = F\big(U_{j-k+1}^n, ..., U_{j+k}^n\big) \tag{2.36}$$

In order to achieve stability, the CFL condition is then extended accordingly with k. For a general $(2k+1)$ scheme with $k \geq 0$,

$$CFL = max\,|f'(u)|\,\frac{\Delta t}{\Delta x} \leq k \tag{2.37}$$

where the function $f(u)$ is any flux function, if otherwise a system of function then $f'(u)$ shall be eigenvalues. Likewise, similar to the conservative scheme, LTS extension for numerical flux form in equation (2.28) is:

$$F_{j+1/2} = \frac{1}{2}(f(U_j^n) + f(U_{j+1}^n)) - \frac{1}{2}\sum_{i=-\infty}^{\infty} Q_{j+1/2}^i (U_{j+1+i}^n - U_{j+i}^n) \tag{2.38}$$

where as flux difference formulation from (2.29) is extended as:

$$U_i^{n+1} = U_i^n - \frac{\Delta t}{\Delta x}\sum_{i=0}^{\infty}\left(A_{j-1/2-i}^{i+}(U_{j+i}^n - U_{j-1+i}^n) + A_{j+1/2+i}^{i-}(U_{j+1+i}^n - U_{j+i}^n)\right) \tag{2.39}$$

Q and A are simply how numerical viscosity and flux difference splitting coefficient provide information to flux function at the interface for every designated i cells away. The domain of dependence of LTS scheme sources from $|i|$, and when $i = 0$ LTS will recover to the standard method in (2.28) and (2.29).

2.5.1 LTS-Godunov

Godunov scheme is a local scheme where it solves for every cell interfaces' Riemann problem. Based on LeVeque's [3] simplification, the generalization of this method describes wave interaction between cells as its *original flux function*. As for LTS-Godunov, it is an extension that encapsulates neighbouring cells' information to update every explicit time step. The following are its viscosity coefficient and flux difference splitting coefficient respectively [6]

Numerical viscosity coefficient:

$$Q^i = \begin{cases} 2\dfrac{\left(f(u) + iu\frac{\Delta x}{\Delta t}\right)_{j+1} - M_{j+1/2}\left(f(u) + iu\frac{\Delta x}{\Delta t}\right)}{u_{j+1} - u_j} & , i < 0 \\ \dfrac{f_j + f_{j+1} - 2M_{j+1/2}\left(f(u) + iu\frac{\Delta x}{\Delta t}\right)}{u_{j+1} - u_j} & , i = 0 \\ 2\dfrac{\left(f(u) + iu\frac{\Delta x}{\Delta t}\right)_{j} - M_{j+1/2}\left(f(u) + iu\frac{\Delta x}{\Delta t}\right)}{u_{j+1} - u_j} & , i > 0 \end{cases} \tag{2.40}$$

Flux difference coefficient:

$$A_{j-1/2-i}^{i+} = \frac{1}{\Delta u_{j-1/2-i}}\left(M_{j-1/2-i}\left(f(u) - (i+1)u\frac{\Delta x}{\Delta t}\right)\right. \tag{2.41a}$$

$$\left. - M_{j-1/2-i}\left(f(u) - iu\frac{\Delta x}{\Delta t}\right) + u_{j-i}\frac{\Delta x}{\Delta t}\right) \tag{2.41b}$$

$$A_{j+1/2+i}^{i-} = \frac{1}{\Delta u_{j+1/2+i}}\left(M_{j+1/2+i}\left(f(u) + iu\frac{\Delta x}{\Delta t}\right)\right. \tag{2.41c}$$

$$\left. - M_{j+1/2+i}\left(f(u) + (i+1)u\frac{\Delta x}{\Delta t}\right) + u_{j+i}\frac{\Delta x}{\Delta t}\right) \tag{2.41d}$$

where the function M for LTS-Godunov shares the M function as the ordinary Godunov scheme defined in (2.31).

2.5.2 LTS-Roe

Similar to LTS-Godunov, LTS-Roe solves for every cell interface as Riemann problem. The difference is that LTS-Roe describes the wave interaction between cells as *linearised flux function*. This also means that extrema or critical points of a linear function are at cell interfaces.

Numerical viscosity coefficient:

$$Q^0 = |\lambda| \tag{2.42a}$$

$$Q^{\mp i} = 2max\left(0, \pm\lambda - i\frac{\Delta x}{\Delta t}\right) \quad for \quad i > 0 \tag{2.42b}$$

Flux difference coefficient:

$$A^{i\pm} = \pm max\left(0, min\left(\pm\lambda - i\frac{\Delta x}{\Delta t}, \frac{\Delta x}{\Delta t}\right)\right) \tag{2.43}$$

where λ is the Rankine-Hugoniot shock speed or eigenvalues for a system of equations. It can also be proven that this scheme is the linearised flux function of LTS-Godunov, $f_{j+1/2}(u) = \hat{A}_{j+1/2}u$. To establish the proof from proposition 11 in Lindqvist [6] for numerical flux in scalar equation.

Prove that the LTS-Roe scheme has a numerical flux of:

$$\begin{aligned} F_{j+1/2} = M_{j+1/2}(f(u)) &- \sum_{i=1}^{\infty}\left[\left(f(u) - i\frac{\Delta x}{\Delta t}u\right)_{j+1-i} - M_{j+1/2-i}\left(f(u) - i\frac{\Delta x}{\Delta t}u\right)\right] \\ &- \sum_{i=1}^{\infty}\left[\left(f(u) - i\frac{\Delta x}{\Delta t}u\right)_{j+i} - M_{j+1/2+i}\left(f(u) - i\frac{\Delta x}{\Delta t}u\right)\right] \end{aligned} \tag{2.44}$$

where function M is:

$$M_{j+1/2}(w(u)) = \begin{cases} \min\limits_{u\in\{U_j, U_{j+1}\}} w(u) & , U_j < U_{j+1} \\ \max\limits_{u\in\{U_j, U_{j+1}\}} w(u) & , U_j \geq U_{j+1} \end{cases}$$

Using the numerical flux function from (2.38) and LTS-Roe numerical viscosity coefficient from (2.42a)

Proof:

$$
\begin{aligned}
F_{j+1/2} &= \frac{1}{2}(f(U_j^n) + f(U_{j+1}^n)) - \frac{1}{2}\sum_{i=-\infty}^{\infty} Q_{j+1/2}^i (U_{j+1+i}^n - U_{j+i}^n) \\
&= \frac{1}{2}(f(U_j^n) + f(U_{j+1}^n)) - \frac{1}{2}\left[\sum_{i=1}^{\infty} 2\max\left(0, -\lambda - i\frac{\Delta x}{\Delta t}\right)\cdot(U_{j+1-i} - U_{j-i})\right. \\
&\qquad \left. + \sum_{i=1}^{\infty} 2\max\left(0, \lambda - i\frac{\Delta x}{\Delta t}\right)\cdot(U_{j+1+i} - U_{j+i}) + |\lambda|(U_{j+1} - U_j)\right] \\
&= \frac{1}{2}(f(U_j^n) + f(U_{j+1}^n)) - \sum_{i=1}^{\infty} \max\left(0, -\lambda - i\frac{\Delta x}{\Delta t}\right)\cdot(U_{j+1-i} - U_{j-i}) \\
&\qquad - \sum_{i=1}^{\infty} \max\left(0, \lambda - i\frac{\Delta x}{\Delta t}\right)\cdot(U_{j+1+i} - U_{j+i}) \\
&\qquad - \frac{1}{2}|\lambda|(U_{j+1} - U_j)
\end{aligned}
$$

scalar, $f = \lambda u$

$$
\begin{aligned}
&= \frac{1}{2}f(U_j^n) + \frac{1}{2}f(U_{j+1}^n) - \frac{1}{2}f(U_{j+1}^n) + \frac{1}{2}f(U_j^n) \\
&\qquad - \sum_{i=1}^{\infty} \max\left(0, \left(f(u) - i\frac{\Delta x}{\Delta t}u\right)_{j+1-i} - \left(f(u) - i\frac{\Delta x}{\Delta t}u\right)_{j-i}\right) \\
&\qquad - \sum_{i=1}^{\infty} \max\left(0, \left(f(u) - i\frac{\Delta x}{\Delta t}u\right)_{j+i} - \left(f(u) - i\frac{\Delta x}{\Delta t}u\right)_{j+1+i}\right)
\end{aligned}
$$

Due to Roe having properties of extrema at cell interfaces,

$$
\begin{aligned}
&= M_{j+1/2}(f(u)) - \sum_{i=1}^{\infty}\left[\left(f(u) - i\frac{\Delta x}{\Delta t}u\right)_{j+1-i} - M_{j+1/2-i}\left(f(u) - i\frac{\Delta x}{\Delta t}u\right)\right] \\
&\qquad - \sum_{i=1}^{\infty}\left[\left(f(u) - i\frac{\Delta x}{\Delta t}u\right)_{j+i} - M_{j+1/2+i}\left(f(u) - i\frac{\Delta x}{\Delta t}u\right)\right]
\end{aligned}
$$

2.5.3 LTS Entropy Condition

A wave in LTS treats whether increasing or decreasing discontinuity with Rankine-Hugoniot condition speed, which is already a correct representation of a shock. Thereafter, LTS does not require any treatment for shock, one does not need to split shock into many discontinuities, and if so, the waves will never merge and shall always travel as separate discontinuities. On the other hand, LTS schemes replace each rarefaction wave simply by introducing entropy-violating shocks that approximate actual rarefaction wave. The rarefaction waves are divided into many discontinuities, sufficiently many discontinuities travelling at different speeds to approximate the true solution.

As the LTS-Roe scheme only accounts for extrema at the boundaries of a linear function, the numerical viscosity coefficients of LTS-Roe and LTS-Godunov schemes

are then equal

$$Q^i_{Roe} = Q^i_{God}$$

when the u is accounting only for the extremum in $R_{j+1/2}$ defined in equation (2.31). Otherwise $Q^i_{God} \geq Q^i_{Roe}$ for all integer i. Subsequently, the entropy violation can be defined generally for the LTS-Roe scheme for cases that be derived as such from

$$f(u) + iu\frac{dx}{dt} = 0$$

The critical points shall be:

$$\begin{aligned} f'(u) + i\frac{dx}{dt} &= 0 \\ f'(u) \cdot \frac{dt}{dx} &= -i\frac{dx}{dt} \cdot \frac{dt}{dx} \\ C_{j+1/2} &= -i \end{aligned}$$

for all i integer and C is the courant number or CFL condition defined in (2.37). This condition also holds true to LTS-Godunov if the critical points u are computed from $f'(u) + i\frac{dx}{dt} = 0$. The critical points are where the exact solution crosses the entropy violating shocks of all LTS-schemes introduced.

Chapter 3

N-Waves Approximation

In this chapter, there shall be an exposition of N-waves approximation and the cohesion of such scheme with LTS schemes, particularly LTS-Godunov and LTS-Roe. The underlying framework of wave approximation has been introduced as 'two/three waves approximation' and 'large time step wave adding scheme' by Qian [9] and Dong [1] respectively. Hereby shall also provide approaches to revise and rationalize these schemes, thus unifying the theories.

3.1 Two/Three-Waves Approximation (Burgers Equation)

A general two-waves approximation introduces wave interaction by splitting into two *linear* discontinuities of a function, an example with burgers flux, $\frac{1}{2}u^2$ with an increasing discontinuity *-1* to *1* suggests an approximation as in figure 3.1.

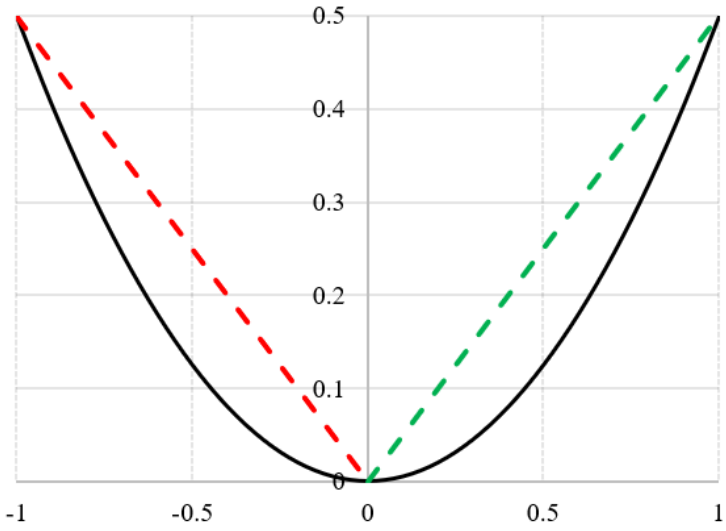

Figure 3.1: Burgers function and two-waves linearised approximation functions

Taking waves with a propagating speed of S in burgers flux. The Rankine-Hugoniot speed will therefore be $S_M = \frac{S_L+S_R}{2}$, where S_L and S_R here are denoted as the left and right rarefaction wave speed. Then the speed of this expansion discontinuity is further split into two speeds. For a Burgers flux the split wave speed will simply be

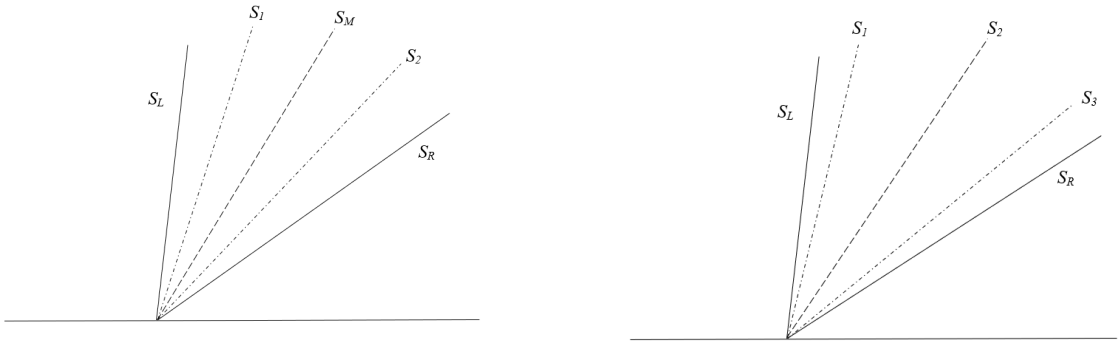

(a) two waves speed (b) three waves speed

Figure 3.2: Two and three waves approximation

the arithmetic average: $S_1 = \frac{S_L+S_M}{2}$ and $S_2 = \frac{S_M+S_R}{2}$. An illustration of two-wave approximation is shown in figure 3.2a.

Similarly for a three-waves approximation, it is essentially further splitting into three parts or functions, subsequently obtaining three separate speeds equally divided. In general for Burgers flux function, two-waves shall have $\frac{1}{4}^{th}$ and $\frac{3}{4}^{th}$ of wave speed entailing the right side of the jump. Whereas a three-waves have $\frac{1}{6}^{th}$, $\frac{1}{2}^{th}$, $\frac{5}{6}^{th}$ of wave speed entailing with regards to three functions respectively. Theoretically, it can extend to more than just two or three waves, however it comes with the cost of computation expense, thus three waves is sufficient to approximate most of the function in this present study. Note that wave approximation is only favourable to a strictly concave or convex function as it exists only as either a maximum or a minimum in a curve. However, a non-convex flux/function does not obey the rule mentioned and is further discussed in later sections.

3.2 Connections with LTS-Roe and LTS-Godunov

LTS-Roe approximates each cell interface by replacing it with a linear function $f = Au$. LTS-Godunov approximates with its original flux function $f = f(u)$. On the other hand, two/three waves approximates by interpolating linear functions into two and three points respectively. A simple illustration is shown in figure 3.3 for Burgers flux. Continuing the discontinuity *-1* to *1* Riemann problem, the Roe scheme will not able to capture the minimum or maximum critical points or one could interpret it such that the Rankine-Hugoniot speed in a Burgers flux is *0* subsequently resulting in a stationary solution. However, for three-waves, it provides a better estimation by 'emulating' the original function as of Godunov. Being said that two and three waves have two and three functions, thereby LTS-Roe can be viewed as a 'one-wave' approximation simply because it takes *one* linear function to connect the discontinuity.

LTS schemes can be viewed as the Godunov scheme applied to a modified flux function [7]. To put into a perspective, the LTS-Roe is viewed as replacing the original $f'(u)$ with *linear flux*:

$$f = \hat{A}u \tag{3.1}$$

while LTS-Godunov is viewed as the original $f'(u)$ replaced with a *quadratic flux*:

$$f = \hat{B}u^2 + \hat{A}u \tag{3.2}$$

the 'LTS-wave addition scheme' in Dong's paper is then interpreted as the equivalent of the LTS-Godunov scheme as $\hat{B}u^2$ variable is active for rarefaction wave. And when $\hat{B} = 0$, it is then reduced to LTS-Roe.

Moving on with the *-1* to *1* jump example. An example of courant number 10.6 and $i = 10$ executed with 100 cells is shown in figure 3.4. Firstly, LTS-Godunov simulates an almost exact solution, proving the best of all schemes. LTS-Roe fails to solve this problem, due to an entropy violation where this supposed rarefaction propagating wave is treated with a Rankine-Hugoniot speed of *0*. On the other hand, the two-waves approximation has one plateau, which suggests a discontinuity induced by two functions. Also, the two gradients that correspond to two wave speeds that are $\frac{1}{4}^{th}$ and $\frac{3}{4}^{th}$. On the other hand, three-waves approximation result in two plateaus which correspond to two discontinuities, entailing three wave speeds that are $\frac{1}{2}^{th}$, $\frac{5}{6}^{th}$.

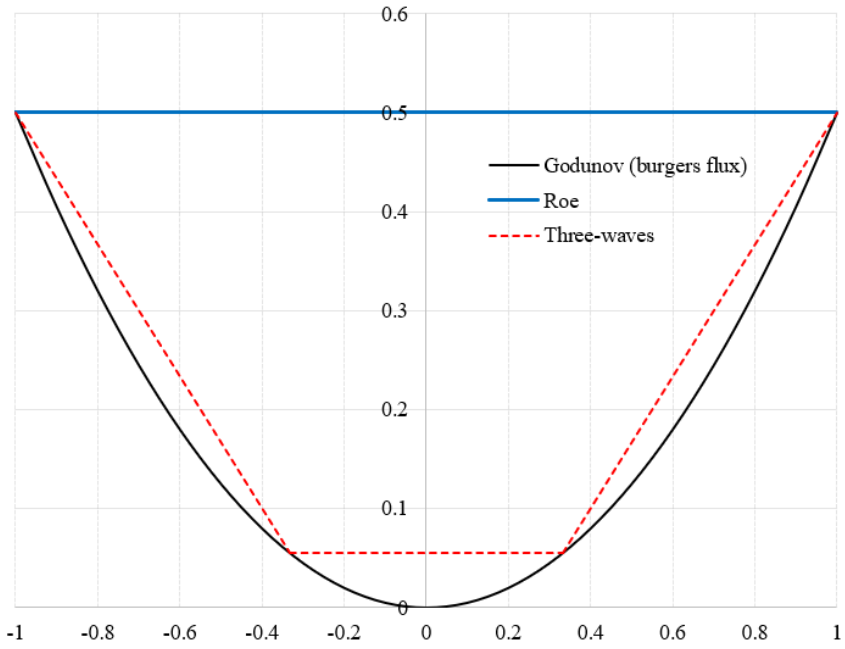

Figure 3.3: LTS-Godunov, LTS-Roe and three-waves linearised approximation functions on Burgers function

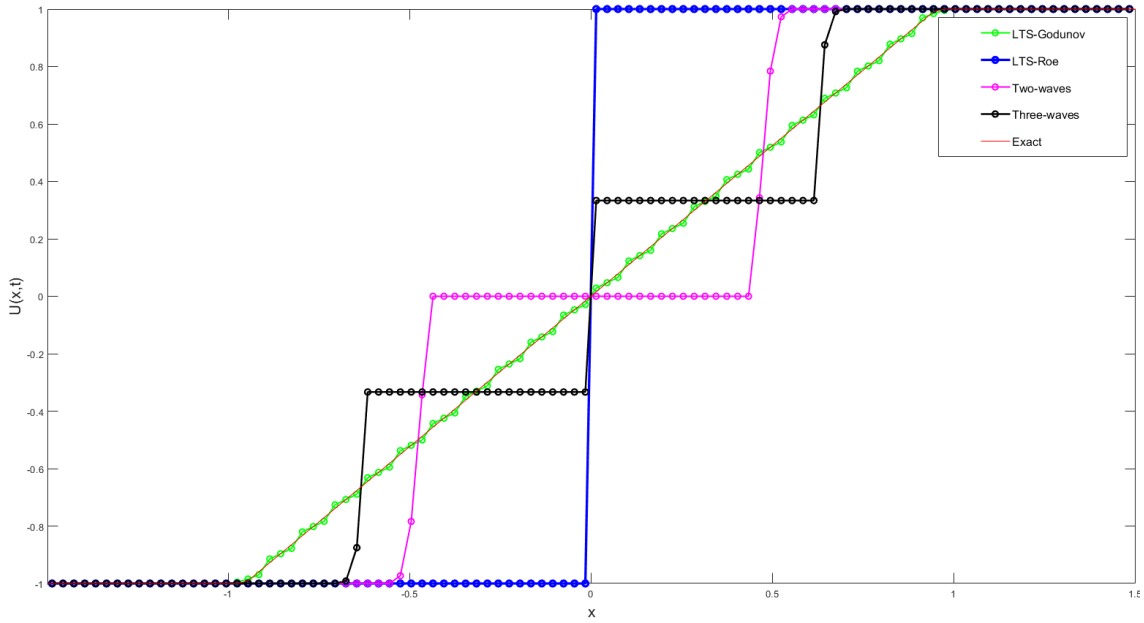

Figure 3.4: Solution comparison for LTS schemes and wave schemes

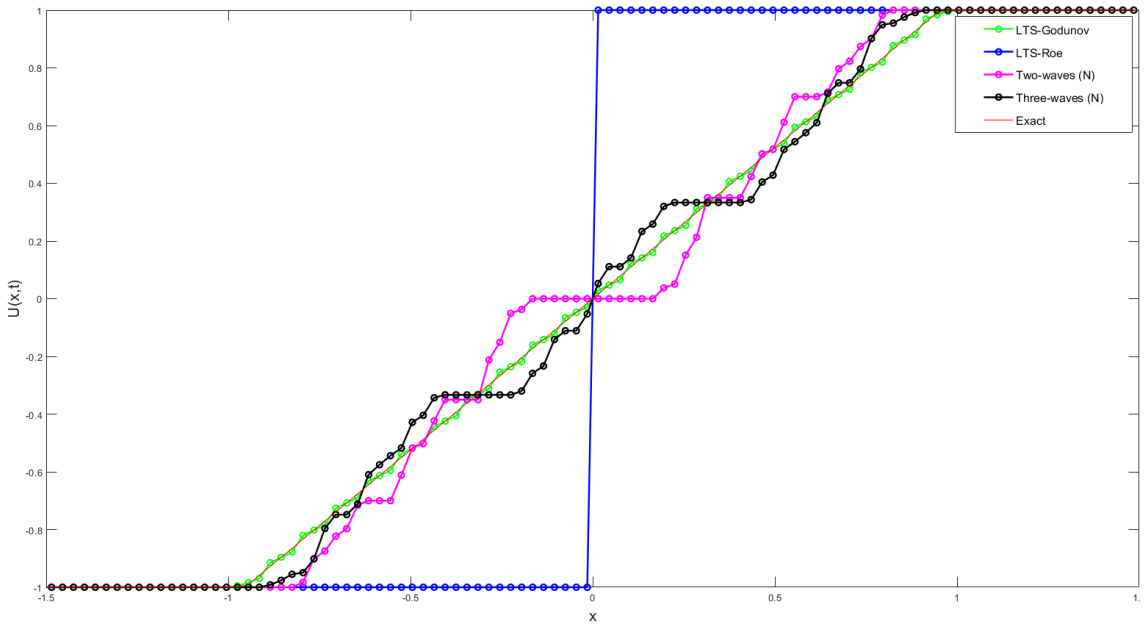

Figure 3.5: Solution comparison for LTS schemes and N-wave schemes

3.3 N-Waves

So far we have discussed, two and three-waves approximation, as well as the connections with LTS-Roe as one-wave. This is the cornerstone of N-waves approximation, by means of N-waves, it is essentially the *infinite waves*. For every increasing discontinuity, the two/three-waves approximation procedure shall be executed rather than having only **one** initial discontinuity from the beginning as discussed in previous sections. Likewise with the LTS scheme, the solution is where discontinuity is split into infinitely many characteristics, gradually approaching the actual flux

function such as LTS-Godunov. To put it in other words, one can view the initial two-waves begin with two linear functions that correspond to one introduced artificial discontinuity. Then, in the next time step, that one artificial discontinuity paves the introduction of two more linear functions, making up to a total of four in the next time step. Subsequently, approaching infinite division of discontinuities - *'infinitely' many joined linear functions*. Figure 3.5 displays the result with the same courant number as the solution in figure 3.4.

3.3.1 Two and Three Waves to N-Approximation Algorithm

To display the approach in obtaining the solution as in figure 3.5, the LTS scheme is used to lay the foundation of the N-approximation, such that the LTS conservation scheme and its numerical viscosity or flux difference coefficient is used to update U_i at each time step simply by modifying the $w(u)$ function in the M function in the general LTS case — LTS-Godunov. Thereby, LTS-Godunov, LTS-Roe, and N-approximation can be solved concurrently.

The following are two-waves and three-waves to N-approximation algorithms for a Burgers flux respectively. Firstly by considering any increasing jump, denoting as u_L to u_R.

Algorithm 1: Two-Waves Approximation (N)

1. For every time step, when $u_L \neq u_R$
2. Construct gradient, m

$$\frac{1}{4}(u_R - u_L) + u_L = m_1$$
$$\frac{3}{4}(u_R - u_L) + u_L = m_2$$

3. Intercepts, a

$$m_1 u_L + a_1 = f(u_L)^*$$
$$a_1 = f(u_L)^* - m_1 u_L$$

$$m_2 u_R + a_2 = f(u_R)^*$$
$$a_2 = f(u_R)^* - m_2 u_R$$

Gives:

$$y_1 = m_1 u + a_1$$
$$y_2 = m_2 u + a_2$$

Here, $f(u)^*$ is the Burgers function.

4. Intersections, solve for u^*

$$m_1 u^* + a_1 = m_2 u^* + a_2$$

5. **if** $u_L < u_R$
   if $u_L \leq u^* \leq u_R$
   Compare u_L, u_R, u^* as variables of function M
   else
   Compare u_L and u_R as variables of function M
   elseif $u_L \geq u_R$
   if $u_R \leq u^* \leq u_L$
   Compare u_L, u_R, u^* as variables of function M
   else
   Compare u_L and u_R as variables of function M

   where function M is defined as 2.31, while revised for LTS as $M\left(f(u) + iu\frac{\Delta x}{\Delta t}\right)$ for viscosity method or the flux difference method as in (2.41)

6. Assigning $f(u)$ in function M

   if $u_L = u_R$
   $f(u)$ is the Burgers function
   else
   if $u < u^*$
   $f(u) = y_1$
   else
   $f(u) = y_2$

Algorithm 2: Three-Waves Approximation (N)

1. For every time step, when $u_L \neq u_R$
2. Construct gradient, m

$$\frac{1}{6}(u_R - u_L) + u_L = m_1$$
$$\frac{1}{2}(u_R - u_L) + u_L = m_2$$
$$\frac{5}{6}(u_R - u_L) + u_L = m_2$$

3. Intercepts, a

$$\begin{aligned} m_1 u_L + a_1 &= f(u_L)^* \\ a_1 &= f(u_L)^* - m_1 u_L \\ m_2\left(\frac{u_R - u_L}{3}\right) + u_L + a_2 &= f\left(\frac{u_R - u_L}{3} + u_L\right)^* \\ a_2 &= f\left(\frac{u_R - u_L}{3} + u_L\right)^* - m_2\left(\frac{u_R - u_L}{3}\right) + u_L \\ m_3 u_R + a_3 &= f(u_R)^* \\ a_3 &= f(u_R)^* - m_3 u_R \end{aligned}$$

   Gives:

$$\begin{aligned} y_1 &= m_1 u + a_1 \\ y_2 &= m_2 u + a_2 \\ y_3 &= m_3 u + a_3 \end{aligned}$$

   Here, $f(u)^*$ is the Burgers function.

4. Intersections, solve for $u*$

$$m_1 u_1^* + a_1 = m_2 u_2^* + a_2$$
$$m_2 u_2^* + a_2 = m_3 u_3^* + a_3$$

5. **if** $u_L < u_R$
   - if $u_L \leq u_1^* \leq u_R$ and $u_R < u_2^*$
     - Compare u_L, u_R and u_1^* as variables of function M
   - elseif $u_L > u_1^*$ and $u_L \leq u_2^* \leq u_R$
     - Compare u_L,u_R, u_2^*, as variables of function M
   - elseif $u_L < u_1^*$ and $u_R > u_2^*$
     - Compare u_L, u_R, u_1^* and u_2^* as variables of function M
   - else
     - Compare u_L and u_R as variables of function M

   elseif $u_L \geq u_R$
   - if $u_R \leq u_1^* \leq u_L$ and $u_R > u_2^*$
     - Compare u_L, u_R and u_1^* as variables of function M
   - elseif $u_L < u_1^*$ and $u_R \leq u_2^* \leq u_L$
     - Compare u_L,u_R, u_2^*, as variables of function M
   - else
     - Compare u_L, u_R, u_1^* and u_2^* as variables of function M

   where function M is defined as in (2.31), while revised for LTS as $M\left(f(u) + iu\frac{\Delta x}{\Delta t}\right)$ for viscosity method or the flux difference method as in (2.41)

Algorithm 2: Three-Waves Approximation (N)

6. Assigning $f(u)$ in function M

if $u_L = u_R$
    $f(u)$ is the Burgers function
else
    if $u \leq u_1^*$
        $f(u) = y_1$
    elseif $u \geq u_2^*$
        $f(u) = y_3$
    else
        $f(u) = y_2$

3.3.2 Weakness

One weakness discovered for the introduced waves-approximation scheme is that it only applies on a Burgers function. As the speed does not translate accordingly on any arbitrary convex, concave or non-convex function such as the Buckley-Leverett function. Subsequently, the linear approximations do not lie above/below (or on) any function. In order to establish a scheme for general wave approximation, thereby requiring a reformulation of the methods introduced by Qian and Dong.

3.3.3 Reformulation

While the introduced proposition by Qian has waves speed as the determinant for the actual function approximation. We suggest that this is no need for the case in the scheme. One could simply construct these artificial waves speed without considering or calculating the wave speed itself. The emulation of the actual flux function or the 'target function' is produced by splitting equidistant points for any existing Riemann problems at any cell interface. To demonstrate that, a proposal of this N-waves algorithm can be achieved by the following algorithms. The former is two-waves proliferate to approaching N-waves, the latter is three-waves proliferate to approaching N-waves. Also, the reformulation shall thus be labelled as 'Two-N-waves approximation' and 'Three-N-waves approximation'.

Algorithm 3: Two-N-Waves Approximation

1. For every time step, when $u_L \neq u_R$
2. Construct intersections, u^*

$$u^* = \frac{u_R - u_L}{2} + u_L$$

3. Construct gradients, m

$$m_1 = \frac{f(u^*) - f(u_L)}{u^* - u_L}$$
$$m_2 = \frac{f(u_R) - f(u^*)}{u_R - u^*}$$

Here, $f(u)$ is the target function.

4. Intersections,

$$a_1 = -m_1 u^* + f(u^*)$$
$$a_2 = -m_2 u^* + f(u^*)$$

Gives:

$$y_1 = m_1 u + a_1$$
$$y_2 = m_2 u + a_2$$

5. **if** $u_L < u_R$
   if $u_L \leq u^* \leq u_R$
   Compare u_L, u_R, u^* as variables of function M
   else
   Compare u_L and u_R as variables of function M
   elseif $u_L \geq u_R$
   if $u_R \leq u^* \leq u_L$
   Compare u_L, u_R, u^* as variables of function M
   else
   Compare u_L and u_R as variables of function M

   where function M is defined as 2.31, while revised for LTS as $M\left(f(u) + iu\frac{\Delta x}{\Delta t}\right)$ for viscosity method or the flux difference method as in (2.41)

6. Assigning $f(u)$ in function M

   if $u_L = u_R$
   $f(u)$ is the target function
   elseif $u_L < u_R$
   if $u < u^*$
   $f(u) = y_1$
   else
   $f(u) = y_2$
   elseif $u_L \geq u_R$
   if $u \leq u^*$
   $f(u) = y_2$
   else
   $f(u) = y_1$

Algorithm 4: Three-N-Waves Approximation

1. For every time step, when $u_L \neq u_R$
2. Construct intersections, u^*

$$u_1^* = \frac{u_R - u_L}{3} + u_L$$
$$u_2^* = \frac{u_R - u_L}{3} + u_1^*$$

3. Construct gradients, m

$$m_1 = \frac{f(u_1^*) - f(u_L)}{u_1^* - u_L}$$
$$m_2 = \frac{f(u_2^*) - f(u_1^*)}{u_2^* - u_1^*}$$
$$m_3 = \frac{f(u_2^*) - f(u_1^*)}{u_R - u_2^*}$$

   Here, $f(u)$ is the target function.

4. Intersections

$$a_1 = -m_1 u_1^* + f(u_1^*)$$
$$a_2 = -m_2 u_2^* + f(u_2^*)$$
$$a_3 = -m_3 u_R + f(u_R^*)$$

   Gives:

$$y_1 = m_1 u + a_1$$
$$y_2 = m_2 u + a_2$$
$$y_3 = m_3 u + a_3$$

5. **if** $u_L < u_R$
   - if $u_L \leq u_1^* \leq u_R$ and $u_R < u_2^*$
     - Compare u_L, u_R and u_1^* as variables of function M
   - elseif $u_L > u_1^*$ and $u_L \leq u_2^* \leq u_R$
     - Compare u_L,u_R, u_2^*, as variables of function M
   - elseif $u_L < u_1^*$ and $u_R > u_2^*$
     - Compare u_L, u_R, u_1^* and u_2^* as variables of function M
   - else
     - Compare u_L and u_R as variables of function M

   elseif $u_L \geq u_R$
   - if $u_R \leq u_1^* \leq u_L$ and $u_R > u_2^*$
     - Compare u_L, u_R and u_1^* as variables of function M
   - elseif $u_L < u_1^*$ and $u_R \leq u_2^* \leq u_L$
     - Compare u_L,u_R, u_2^*, as variables of function M
   - else
     - Compare u_L, u_R, u_1^* and u_2^* as variables of function M

   where function M is defined as in (2.31), while revised for LTS as $M\left(f(u) + iu\frac{\Delta x}{\Delta t}\right)$ for viscosity method or the flux difference method as in (2.41)

Algorithm 4: Three-N-Waves Approximation

6. Assigning $f(u)$ in function M

if $u_L = u_R$
    $f(u)$ is the target function
elseif $u_L < u_R$
    if $u \leq u_1^*$
        $f(u) = y_1$
    elseif $u \geq u_2^*$
        $f(u) = y_3$
    else
        $f(u) = y_2$
elseif $u_L \geq u_R$
    if $u \leq u_2^*$
        $f(u) = y_3$
    elseif $u \geq u_1^*$
        $f(u) = y_1$
    else
        $f(u) = y_2$

3.4 Buckley-Leverett Equation

We have discussed LTS-schemes as well as N-waves approximation that strictly apply to concave or convex function, and we are interested in discovering the more complicated non-convex function. It was discussed in section 2.2.2 that when f is convex or concave, we expect the solution to the Riemann problem to be always a shock or rarefaction wave. As for a non-convex function such as the Buckley-Leverett equation, it involves both the correct entropy solution — shock and rarefaction wave. Thereby, we investigate the characteristics of this equation and its approach in solving with LTS-Godunov, LTS-Roe, and N-waves approximation. Considering a scalar model, in a one-dimensional space the Buckley-Leverett fractional flow function is defined as,

$$f(u) = \frac{k_{rw}(u)}{k_{rw}(u) + Mk_{ro}(u)} \tag{3.3a}$$

$$= \frac{u^2}{u^2 + M(1-u)^2} \tag{3.3b}$$

where M is the viscosity ratio of water to oil or more generally non-wetting fluid to wetting fluid, $M = \mu_w/\mu_o$. Normalized Corey type relative permeabilities, expressed as $k_{rw}(u) = u^{nw}$ and $k_{ro}(u) = u^{no}$. The physical properties, albeit important, are not the best of interest in this study. Therefore we shall focus on investigating the equation as an increasing non-convex function from $f(0) = 0$ to $f(1) = 1$.

3.4.1 Compound Waves

Buckley-Leverett fractional flow equation contains an inflection point, thus the wave connecting the discontinuity will be a shock, rarefaction or combination of the two. To further understand the characteristics and solution of Riemann problem of the fractional flow equation, consider $\gamma(t)$ — a smooth path in space-time that its derivative is continuous (see figure 3.6). Then speed is defined with regards to this path

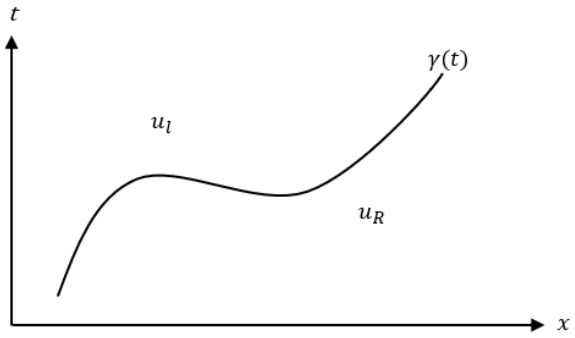

Figure 3.6: 'smooth' path in space time

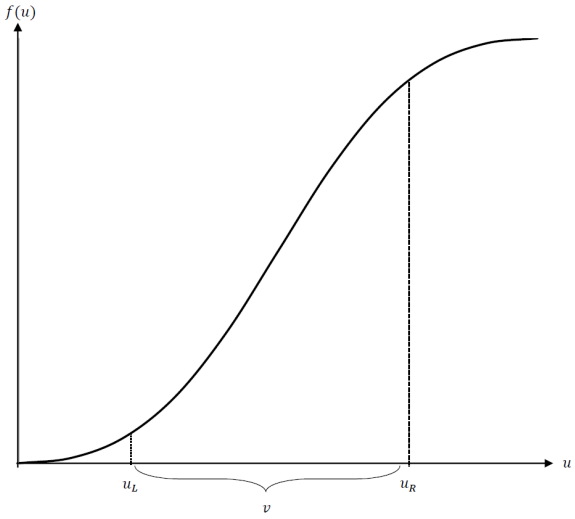

Figure 3.7: Buckley-Leverett function

where $S(t) = \gamma'(t)$. Then let $u(x,t)$ be a weak solution in the form of:

$$u(x,t) = \begin{cases} u_L & , x < \gamma(t) \\ u_R & , x > \gamma(t) \end{cases} \tag{3.4}$$

where $u_L \neq u_R$ (a jump). Then the Rankine-Hugoniot condition is thereby $S(t) = (f(u_L) - f(u_R))/(u_L - u_R)$. The characterization of a valid jump (u_L, u_R) for all v between a u_L and u_R as shown in figure 3.8 such that $\frac{f(v)-f(u_L)}{v-u_L} \geq S(t) \geq \frac{f(v)-f(u_R)}{v-u_R}$. It will also be true for a valid jump for any concave or convex function, Lax entropy condition is obeyed such that $f'(u_L) \geq S(t) \geq f'(u_R)$. Lastly, the solution for this non-convex Riemann problem will thus be connecting the points $(u_L, f(u_L))$ and $(u_R, f(u_R))$ depending on either increasing $(u_L < u_R)$ or decreasing jump $(u_L > u_R)$ as illustrated in figure 3.8a. If $(u_L < u_R)$, then the chord/line connecting is below the graph of f, a lower concave envelope, where the rarefaction wave lies on f until the tangency of the curve otherwise known as the concave hull, then a straight line segment after the tangency is thereby the shock solution. Conversely, if $(u_L > u_R)$, the chord/line connecting is above the graph of f, an upper concave envelope, a straight line segment connecting from the left to the tangency or the convex hull is thereby shock solution, follow by rarefaction lying on f function. On the other hand, if $u_L > u_R$, then $f'(u_L) > f'(u_R)$, the left wave propagates faster than the right, the wave characteristics of such can be seen as in figure 3.8b [5], a shock is expected

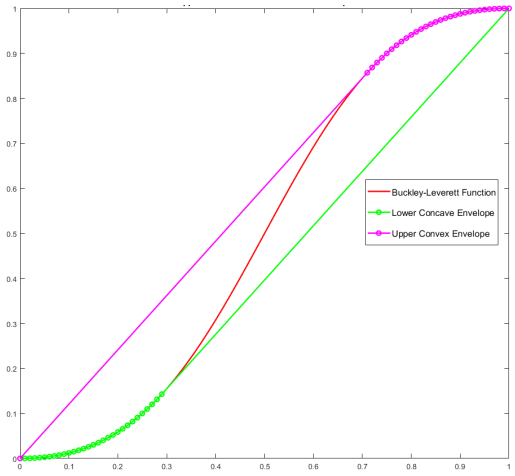

(a) Lower concave envelope and upper convex envelope

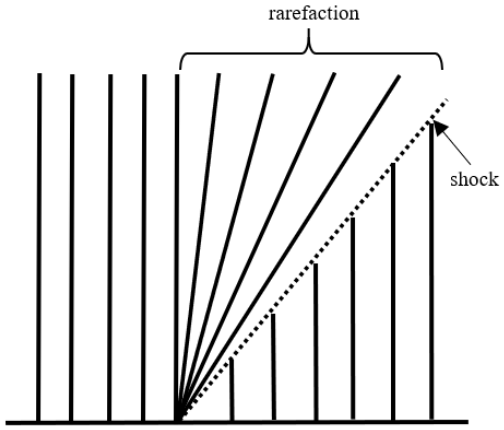

(b) Buckley-Leverett wave characteristics

Figure 3.8: Analysis of Buckley-Leverett riemann problem

just after rarefaction wave propagated. Henceforth, for a non-convex function such as Buckley-Leverett, the solution gives rise to shockwave and rarefaction regardless of whether the jump is increasing or decreasing. This knowledge is crucial for later in solving a non-convex equation with LTS.

Chapter 4

Numerical Simulation

Hereby we present the numerical simulation and the evaluation of results as well as the approach to solving different numerical schemes from ordinary Godunov scheme to LTS-schemes to N-waves approximation scheme of which sets the groundwork to take on the non-convex function — Buckley-Leverett function. Also, the numerical simulations are reproductions of some of the tests from Qian and Dong's papers [1] [9].

4.1 Godunov

As a non-linear test problem, we shall consider Burger's equation $\partial_t u + \partial_x \left(\frac{u^2}{2}\right)$ where shockwave and rarefaction propagation present with the initial data:

$$u_0(x) = \begin{cases} -1 & , x < -1 \\ 0 & , -1 \leq x \leq 1 \\ -1 & , x > 1 \end{cases} \tag{4.1}$$

In figures 4.1 and 4.2 the increasing jump from -1 to 0 display some numerical diffusion for both courant numbers 0.2 and 0.7, having severe diffusion when the time step is lowered. However, as the courant number increases, the solution becomes closer to the exact solution, introducing less numerical diffusion. As for both cases, the decreasing jump from 0 to -1 show very similar result, although it has a good result, it still does not have a good approximation where the exact solution is not smooth.

4.2 LTS-Roe

Considering the Burger's equation with a Riemann problem:

$$u_0(x) = \begin{cases} 0 & , x < 0 \\ 1 & , x \geq 0 \end{cases} \tag{4.2}$$

Figure 4.3 shows the numerical solution with different courant numbers using the LTS-Roe scheme. When courant number ≤ 1, we see that the scheme successfully resolves the rarefaction, however with a little numerical diffusion at courant $= 0.5$. As the courant number exceeds 1, it leads to a similar pattern of entropy violation.

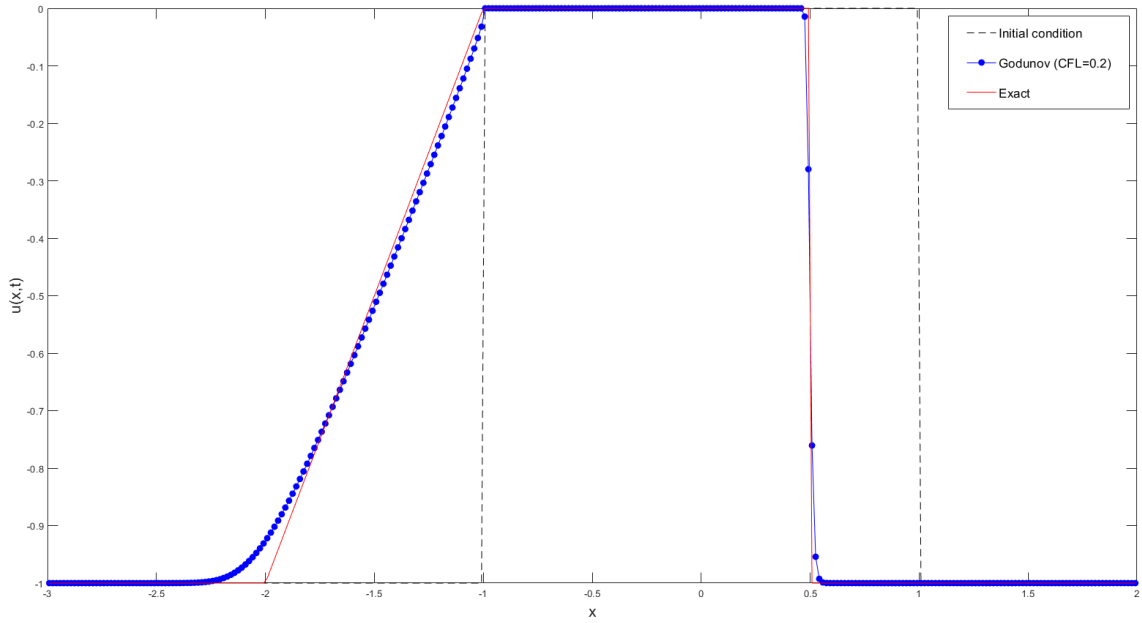

Figure 4.1: Godunov scheme for the Burger's equation at $t = 1$ with courant number 0.2, $dx = 0.0167$, $dt = 0.0033$ and 300 grid cells.

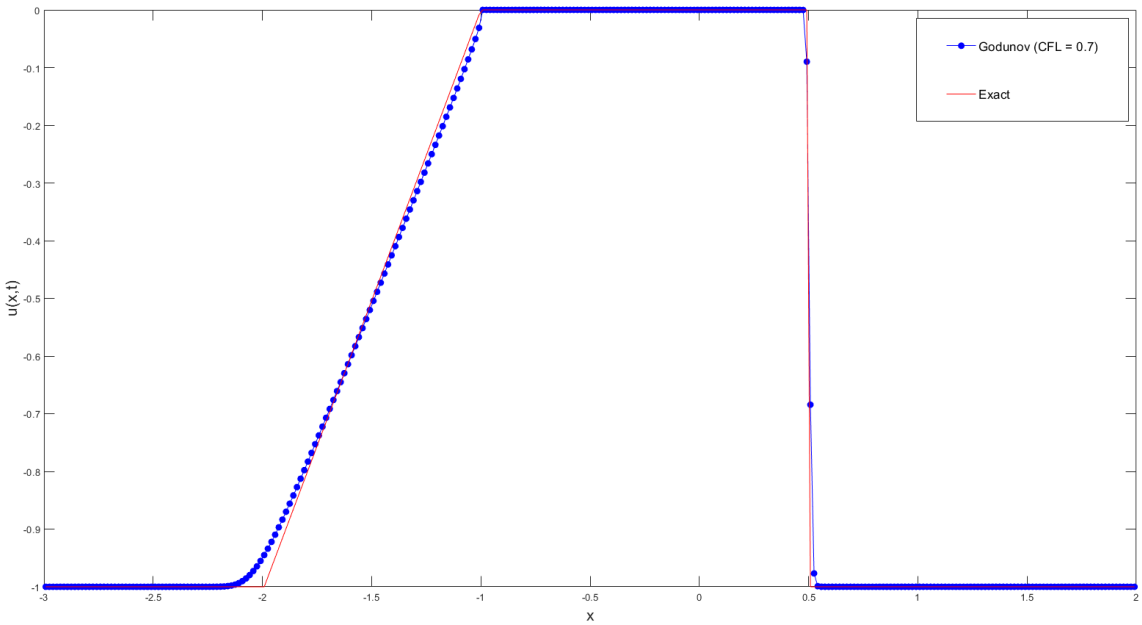

Figure 4.2: Godunov scheme for the Burger's equation at $t = 1$ with courant number 0.7, $dx = 0.0167$ and $dt = 0.0117$ and 300 grid cells.

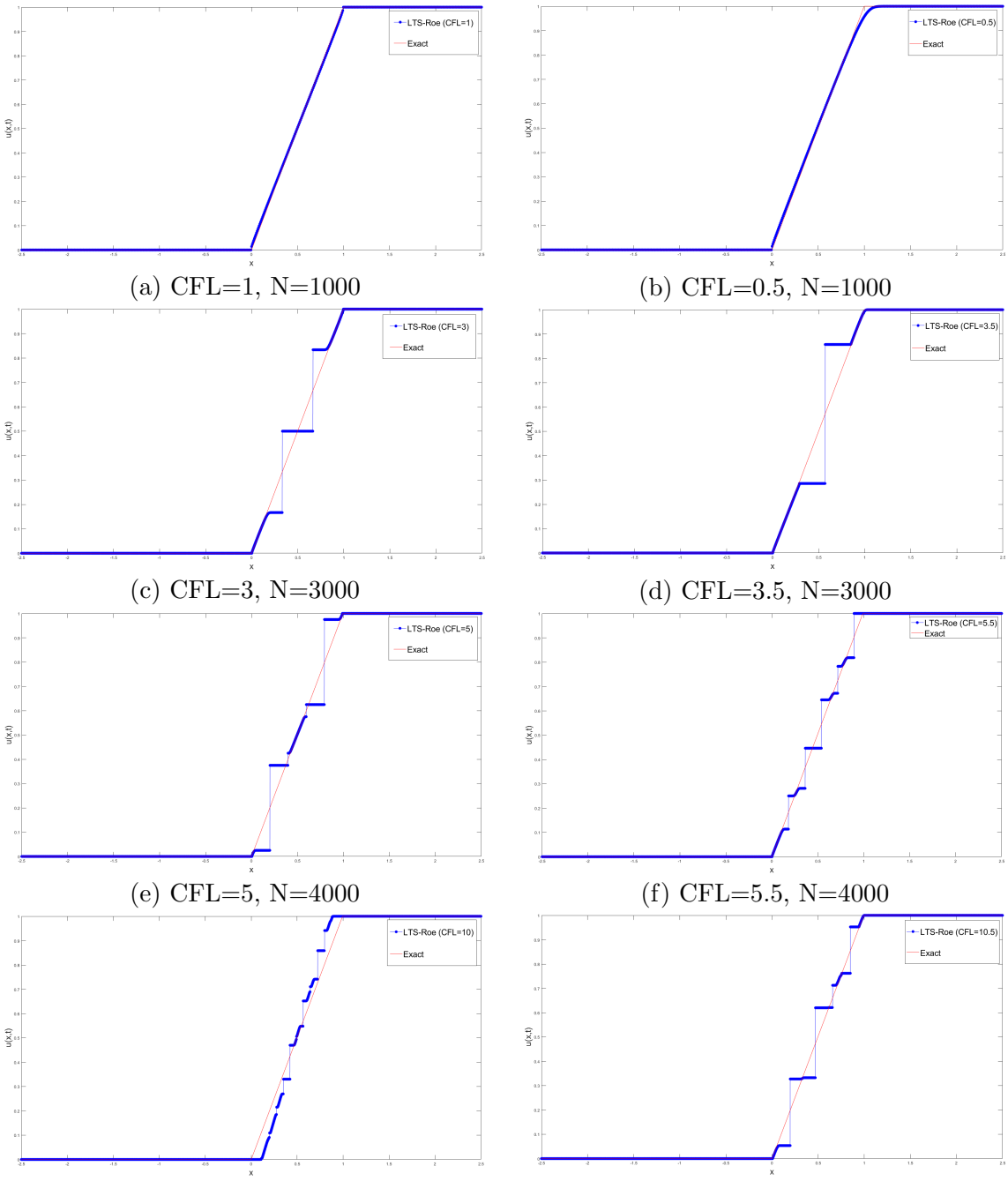

(a) CFL=1, N=1000 (b) CFL=0.5, N=1000

(c) CFL=3, N=3000 (d) CFL=3.5, N=3000

(e) CFL=5, N=4000 (f) CFL=5.5, N=4000

(g) CFL=10, N=8000 (h) CFL=10.5, N=8000

Figure 4.3: LTS-Roe rarefaction solution at different courant number for initial data (4.2)

4.2.1 Transonic Rarefaction

In the case where $f'(u_j) < 0 < f'(u_{j+1})$, we consider Burger's equation with the Riemann problem:

$$u_0(x) = \begin{cases} -1 & , x < 0 \\ 1 & , x \geq 0 \end{cases} \tag{4.3}$$

We see that despite having different courant numbers, the solution remains the same and stationary as it is with the initial condition. This is explained by the entropy violation, as we expect the transonic rarefaction of exact solution to be

a rarefaction wave. In this case, the LTS-Roe scheme has a wave propagating at velocity $a_{j+1/2} = 0$, thus treating it as a stationary shock. Not only does it violates the LTS-Roe entropy, but it also violates the standard Roe entropy.

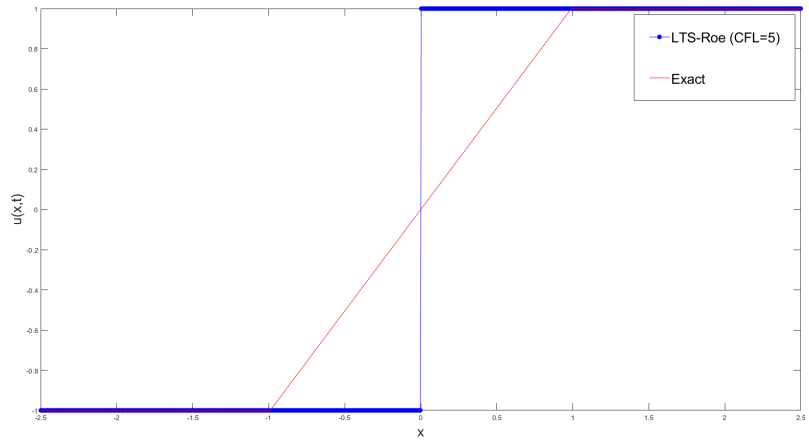

(a) CFL=5, N=1000

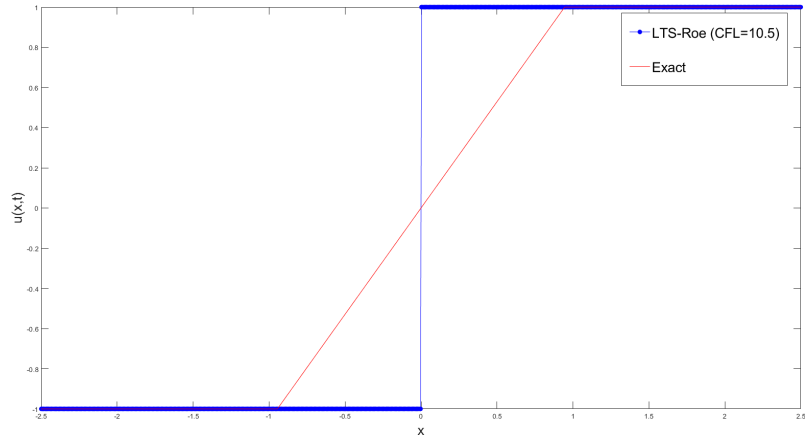

(b) CFL=10.5, N=1000

Figure 4.4: LTS-Roe rarefaction solution at different courant number for initial data (4.3)

4.2.2 Systems of Equations

There has been a lot of development towards producing scalar LTS solutions but not in the view of systems of equations. Thus, hereby we solve a 2x2 system known as the shallow water equations:

$$\frac{\partial h}{\partial t} + \frac{\partial}{\partial x}(hu) = 0 \tag{4.4a}$$

$$\frac{\partial}{\partial t}(hu) + \frac{\partial}{\partial x}(hu^2 + \frac{1}{2}gh^2) = 0 \tag{4.4b}$$

with the initial condition:

$$h_0(x) = \begin{cases} 2 & , x < 0 \\ 1 & , x \geq 0 \end{cases} \tag{4.5a}$$

$$u_0(x) = 0 \tag{4.5b}$$

treating the boundary condition to be *reflective*, such that velocity, u is negative at the boundaries and all designated i corresponding to left and right side of the ghost cells. By solving the Roe matrix of shallow water equation, that is :

$$\begin{pmatrix} 0 & 1 \\ g\hat{h} - \hat{u}^2 & 2\hat{u}^2 \end{pmatrix} \tag{4.6}$$

where

$$\hat{h} = \frac{1}{2}(h_L + h_R)$$
$$\hat{u} = \frac{\sqrt{h_L}u_L + \sqrt{h_R}u_R}{\sqrt{h_L} + \sqrt{h_R}}$$

then, since this is a system of equation, the eigenvalues of the Roe matrix shall be λ in:

Numerical viscosity form:

$$\omega^0 = |\lambda| \tag{4.7a}$$
$$\omega^{\mp i} = 2max\left(0, \pm\lambda - i\frac{\Delta x}{\Delta t}\right), \qquad i > 0 \tag{4.7b}$$

Flux difference form:

$$\Lambda^{i\pm} = \pm max\left(0, min\left(\pm\lambda - i\frac{\Delta x}{\Delta t}, \frac{\Delta x}{\Delta t}\right)\right) \tag{4.7c}$$

the numerical coefficient, $Q^i_{j+1/2}$ and flux difference coefficient, $A^{i\pm}_{j+1/2}$ is then:

$$Q^i_{j+1/2} = \left(\hat{R}\Omega^i\hat{R}^{-1}\right)_{j+1/2} \tag{4.8a}$$

where

$$\Omega^i = diag(\omega^i_1, \omega^i_2) \tag{4.8b}$$

and

$$A^{i\pm}_{j+1/2} = \left(\hat{R}\Phi^{i\pm}\hat{R}^{-1}\right)_{j+1/2} \tag{4.8c}$$

where

$$\Phi^{i\pm} = diag(\Lambda^{i\pm}_1, \Lambda^{i\pm}_2) \tag{4.8d}$$

In figure 4.5, it displays the height and velocity of the solution after $t = 10$. The height refers to the height of the water, and velocity being the velocity of water travelling left and right of the x domain. The solution at CFL= 0.4 and CFL= 1 has the 'smoothest' lines, presenting the better solution. As the courant number increases above 1 and enters the LTS scheme, although the oscillation gradually becomes more apparent, especially at CFL= 20.5, the solution becomes 'step-like', suggesting some entropy violation in LTS-schemes.

As time progresses to $t = 10$ in figure 4.6, it shows the reflected height of the waves, as perceived once courant number exceeds 1 the solution also shows the behaviour of increasing oscillation.

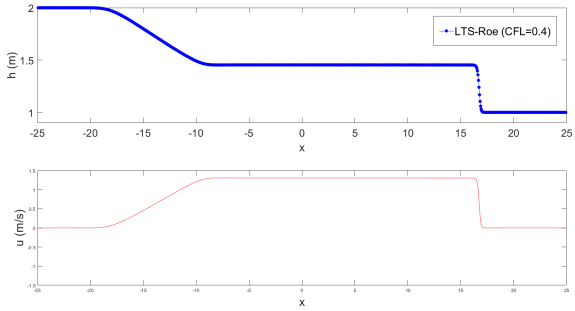

(a) CFL=0.4, N=1000

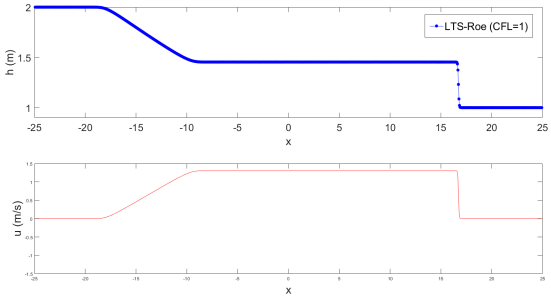

(b) CFL=1, N=1000

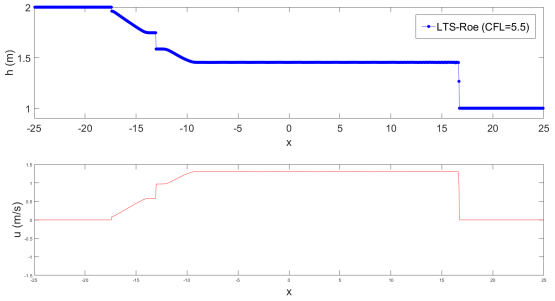

(c) CFL=5.5, N=1000

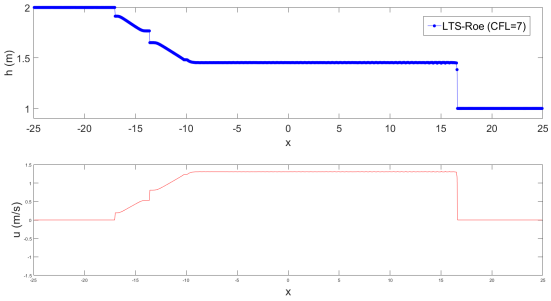

(d) CFL=7, N=1000

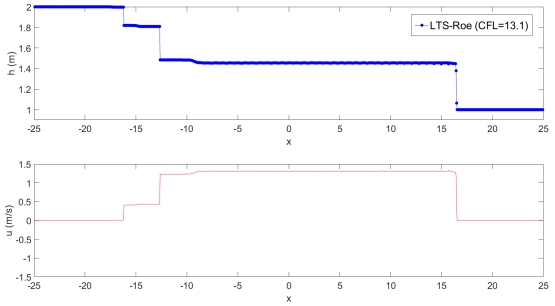

(e) CFL=13.1, N=1000

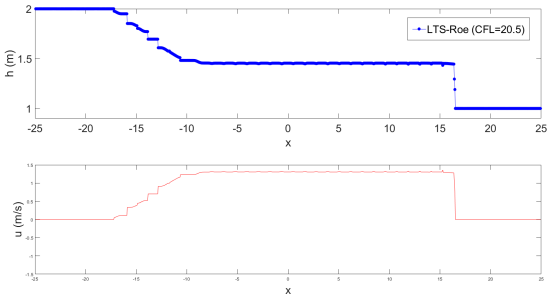

(f) CFL=20.5, N=1000

Figure 4.5: LTS-Roe system solution at $t = 4$

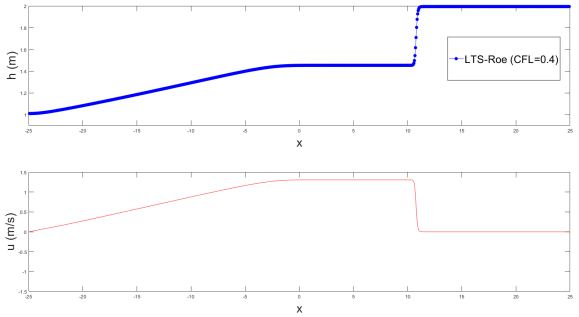

(a) CFL=0.4, N=1000

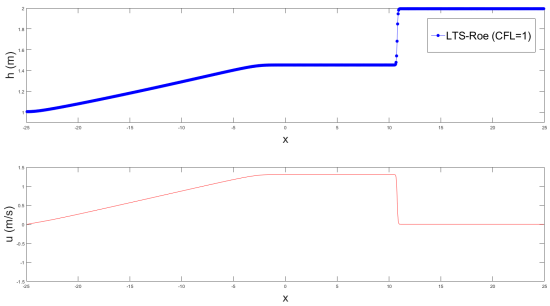

(b) CFL=1, N=1000

Figure 4.6: LTS-Roe system solution at t=10

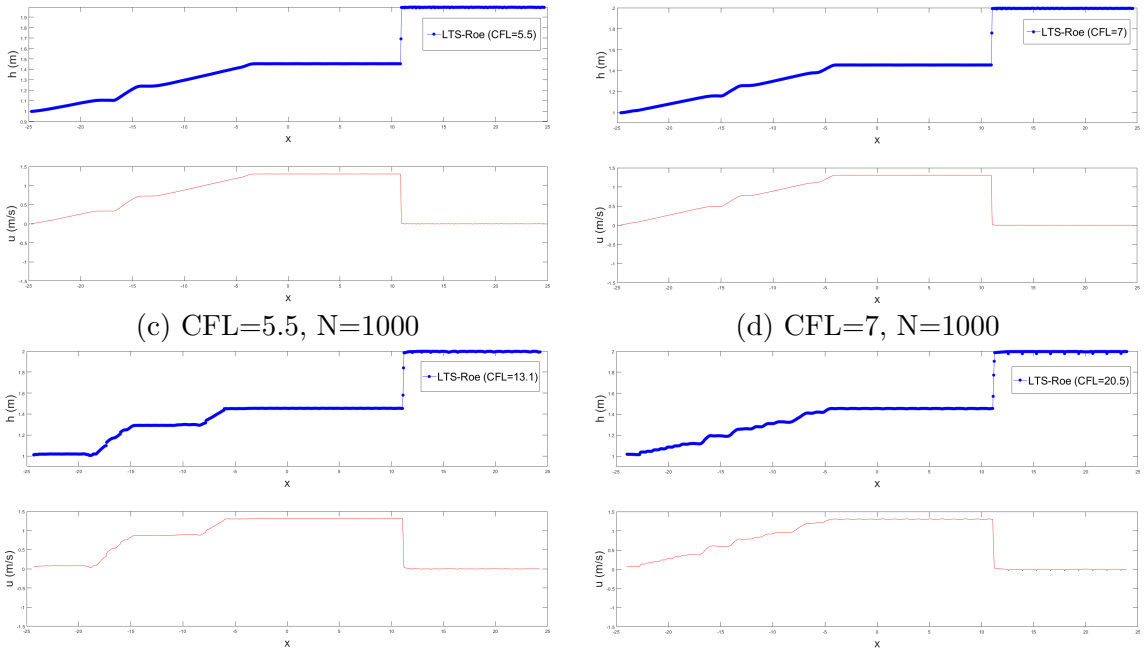

(c) CFL=5.5, N=1000 (d) CFL=7, N=1000

(e) CFL=13.1, N=1000 (f) CFL=20.5, N=1000

Figure 4.6: LTS-Roe system solution at $t = 10$ (*cont.*)

4.3 Test 1 (Scalar Conservation Law in One Dimension)

Test 1 of the numerical experiment that was performed by Dong [1], it was later found that the equation and parameters are formulated by Jiang and Shu [2] and in this study it is used to implement LTS-Roe in comparison towards the LTS-WA (wave addition) in the paper. The problem is a linear equation of scalar conservation law in one-dimensional space such that:

$$u_t + u_x = 0 \qquad , -1 \leq x \leq 1, \qquad t \in (0, 8] \tag{4.9a}$$

$$u_0(x) = nu_0(x) \qquad , \text{periodic} \tag{4.9b}$$

where

$$u_0(x) = \begin{cases} \frac{1}{6}\left(G(x, \beta, z-\delta) + G(x, \beta, z+\delta) + 4G(x, \beta, z)\right) & , -0.8 \leq x \leq -0.6 \\ 1 & , -0.4 \leq x \leq -0.2 \\ 1 - |10(x - 0.1)| & , 0 \leq x \leq 0.2 \\ \frac{1}{6}\left(F(x, \alpha, a-\delta) + F(x, \alpha, a+\delta) + 4F(x, \alpha, a)\right) & , 0.4 \leq x \leq 0.6 \\ 0, & , \text{otherwise} \end{cases}$$

$$G(x, \beta, z) = e^{-\beta(x-z)^2}$$

$$F(x, \alpha, a) = \sqrt{\max(1 - \alpha^2(x-a)^2, 0)}$$

The constants $a = 0.5$, $z = -0.7$, $\delta = 0.005$, $\alpha = 10$ and $\beta = \frac{\ln(2)}{36\sigma^2}$. The solutions are computed up to $t = 0.8$ and at different CFL as shown in figure below:

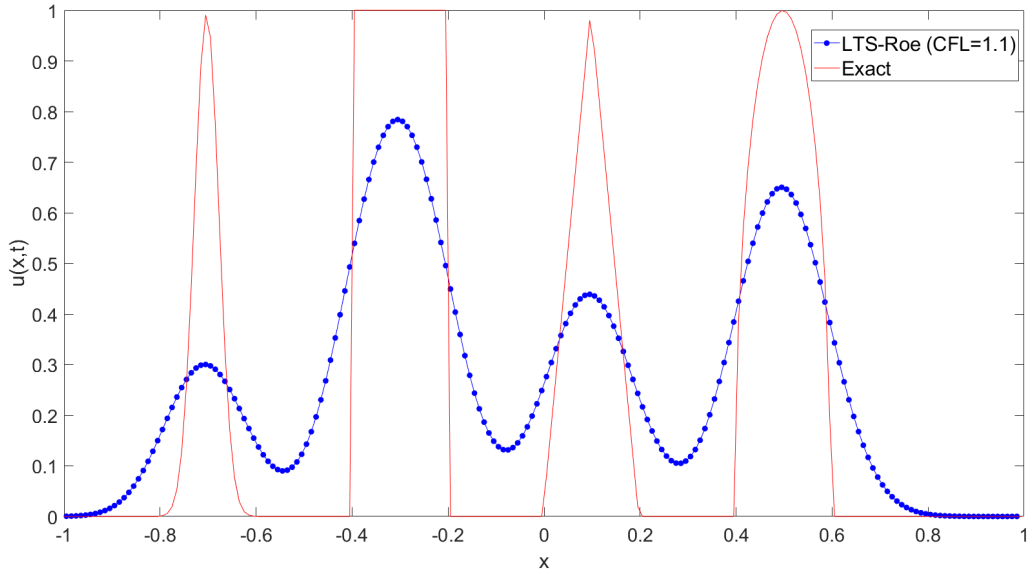

(a) LTS-Roe, CFL=1.1, N=200

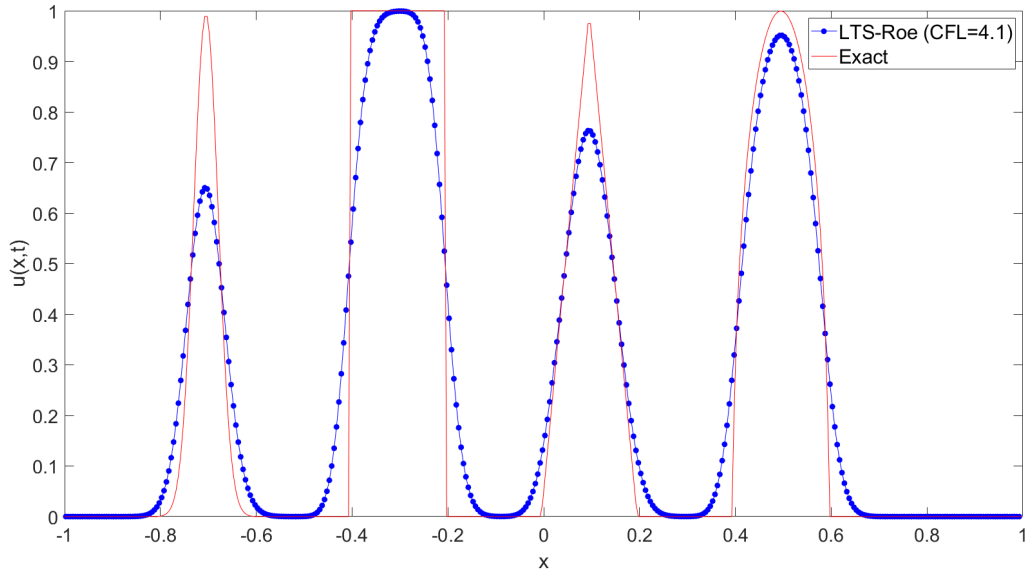

(b) LTS-Roe, CFL=4.1, N=400

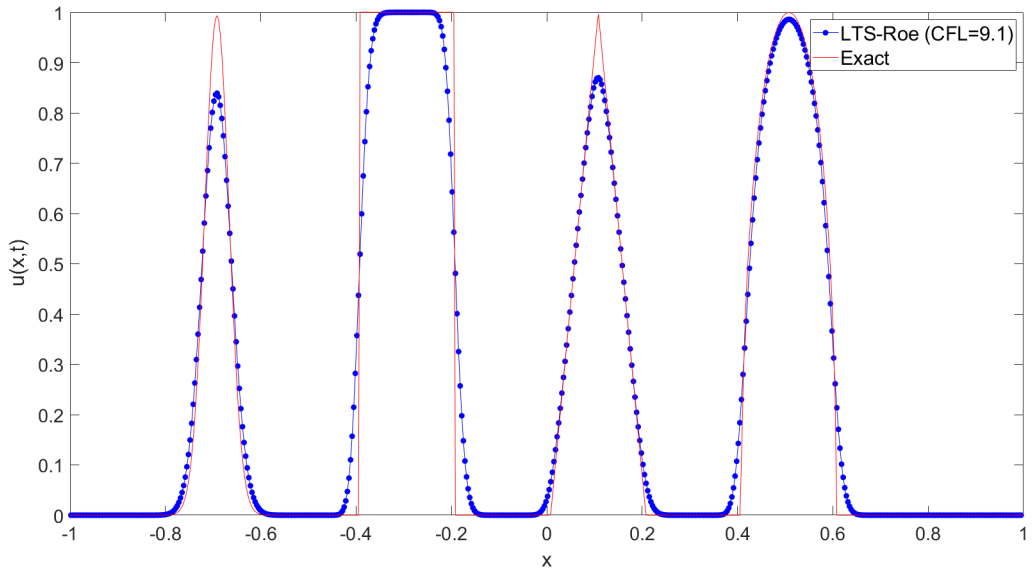

(c) LTS-Roe, CFL=9.1, N=600

Figure 4.7: LTS-Roe solution for initial data 4.9

As a linear equation generates the exact solution when the courant number is an integer, the tests are produced in a random non-integer courant number. There is a considerable amount of numerical diffusion when CFL=1.1, and as the courant number increases the resolution increases and the dissipation decreases at sharp discontinuities. In comparison with Dong's paper (see Appendix A (Dong's Test 1 Figure 9 [1])), the results of the LTS-Roe scheme are comparably identical to the LTS-WA scheme, thus under the linear scalar equation condition, both schemes essentially produce the same result.

4.4 Test 2 (Non-Linear Equation)

Reproducing test 2 of the numerical experiment by Dong [1]. A one-dimensional Burgers equation problem that involves an increasing and decreasing discontinuity. The initial condition is as:

$$u_t + \left(\frac{u^2}{2}\right)_x = 0 \qquad t \in (0, 0.3] \tag{4.10a}$$

$$u_0(x) = \begin{cases} 1 & , -\frac{1}{3} \leq x \leq \frac{1}{3} \\ -1 & , \text{otherwise} \end{cases} \tag{4.10b}$$

Figure 4.8 shows the result. In this test, LTS-Godunov manages to capture the rarefaction wave and shock wave accurately. When CFL=1, there is one distinct discontinuity at the increasing jump, and as the courant number increases, increasingly more discontinuities are present, thus making the wave seem to be more 'seamless' as seen when CFL=9. This is also comparable to the LTS-WA introduced in Dong's paper (see Appendix B (Dong's Test 2 Figure 10 [1])) as the results are identical between LTS-Godunov and LTS-WA. Also, in comparison with LTS-Roe is as expected to not able to solve the transonic wave whereby the zero speed leads to a non-physical discontinuity that violates entropy condition.

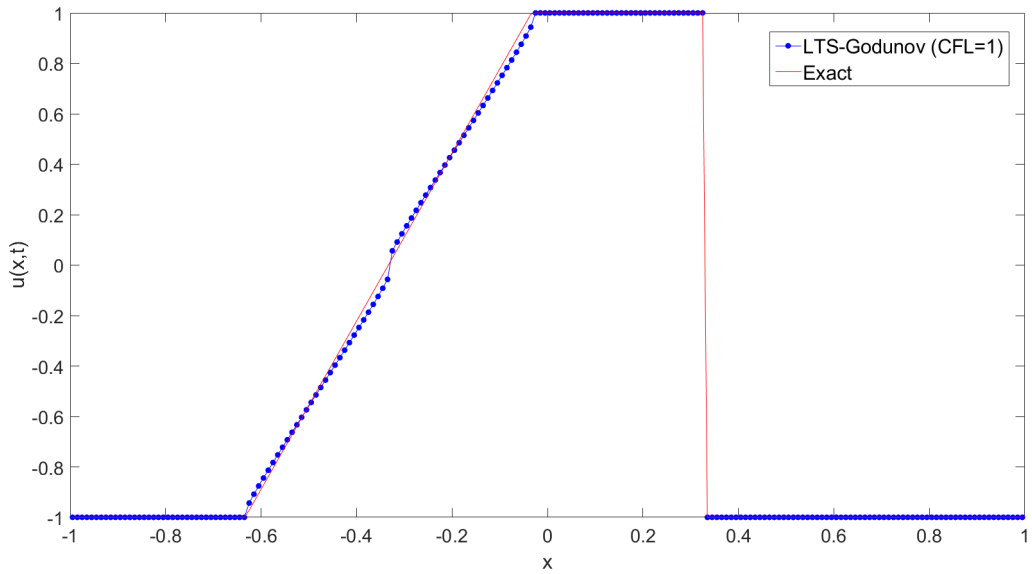

(a) LTS-Godunov, CFL=1, N=200

Figure 4.8: LTS-Godunov solution for initial data 4.10

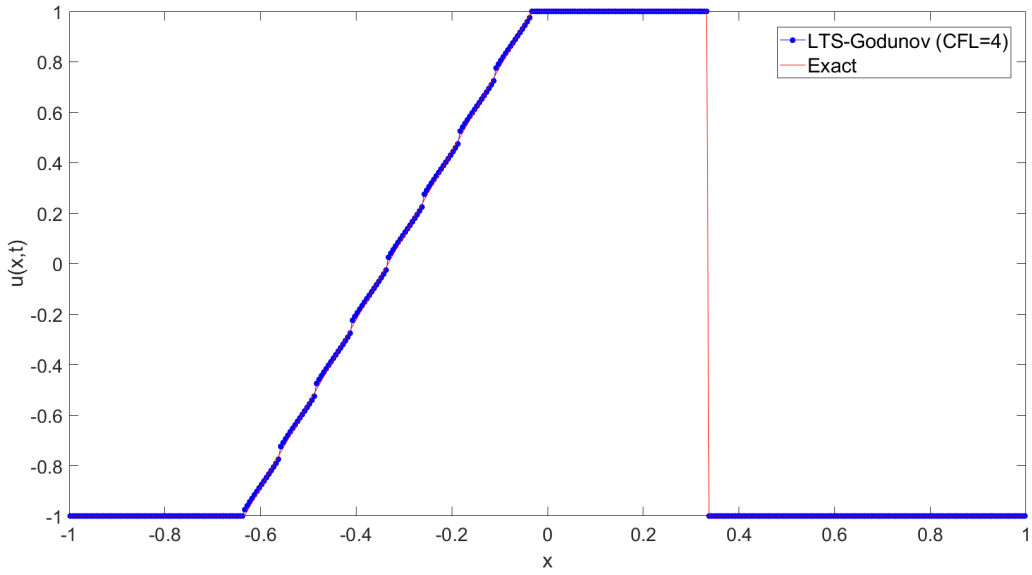

(b) LTS-Godunov, CFL=4, N=400

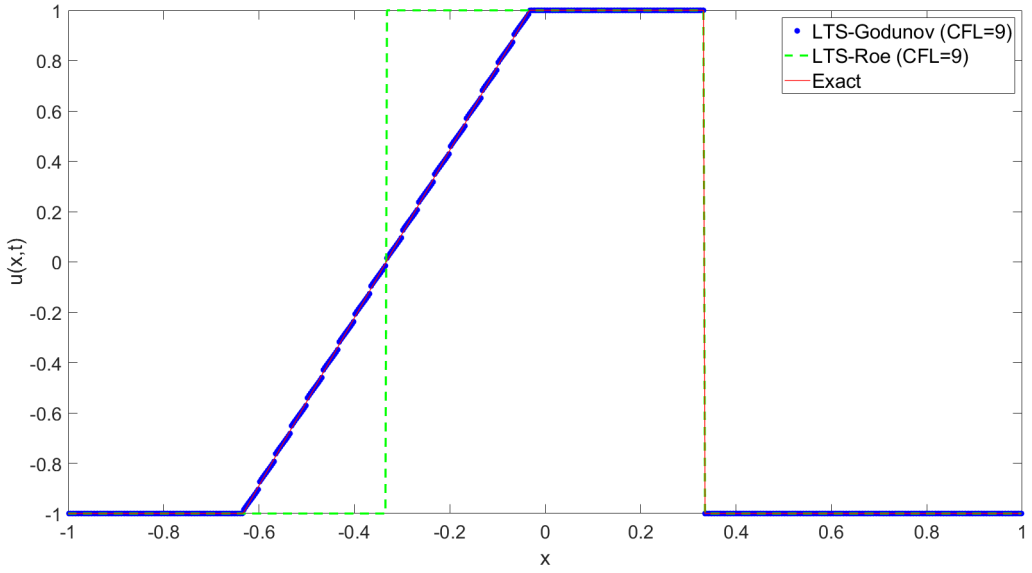

(c) LTS-Godunov and LTS-Roe, CFL=9, N=600

Figure 4.8: LTS-Godunov solution for initial data 4.10 (*cont.*)

4.5 Test 3 (Three-N-Waves Approximation)

Reusing the initial data from test 2 of 4.10, test 3 is conducted to reproduce the multi-wave approximation that was done in Dong's paper (see Appendix C (Dong's Test 2 Figure 11 [1])). The result is shown in figure 4.9. We see that for CFL=1, there exists a discontinuity at the midsection and is almost identical to LTS-Godunov. As the courant number increases, though three-N-waves appx. gives an accurate result, it displays an increasingly zig-zag behaviour at -1 to 1 jump. On the other hand, LTS-Godunov has a smoother approximation compared to three-N-waves. The most obvious comparison shall be when CFL=15, there are two leveled plateaus for three-N-waves approximation, which is a strong evidence of similarity towards LTS-WA in Dong's paper, thus verifying that the three-N-waves method that was developed is valid towards the LTS-WA scheme.

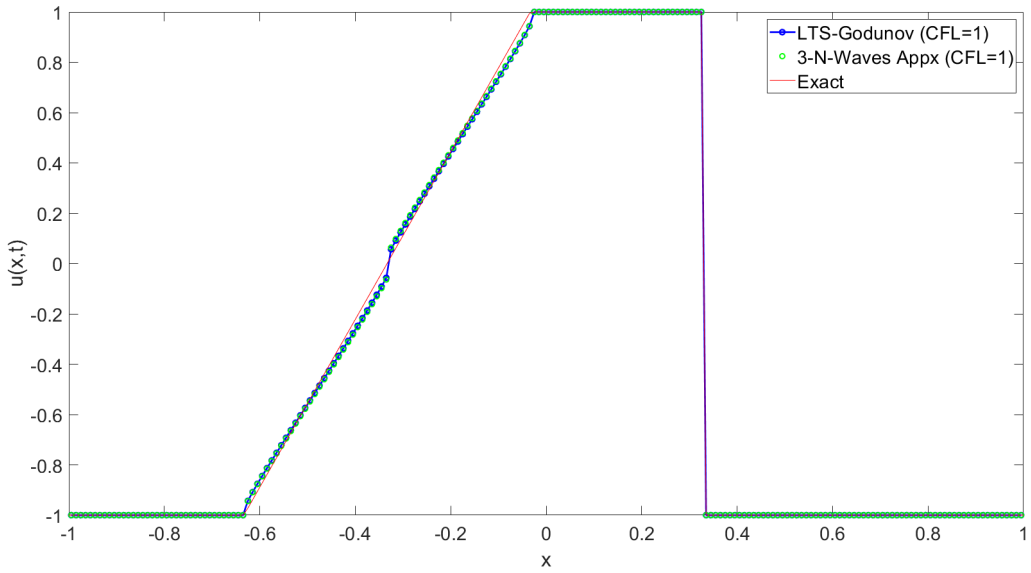

(a) Three-N-waves and LTS-Godunov, CFL=1, N=200

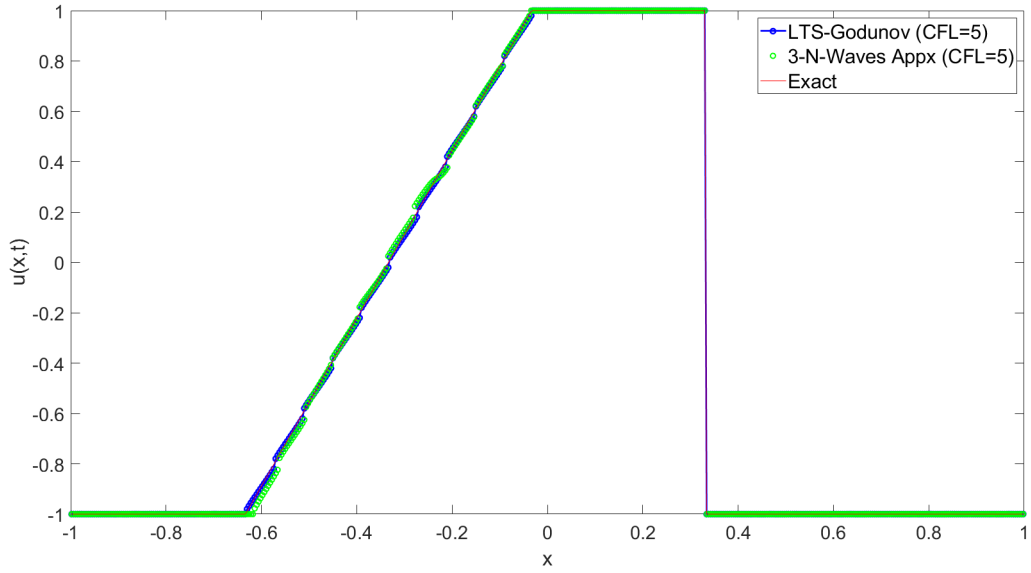

(b) Three-N-waves and LTS-Godunov, CFL=5, N=500

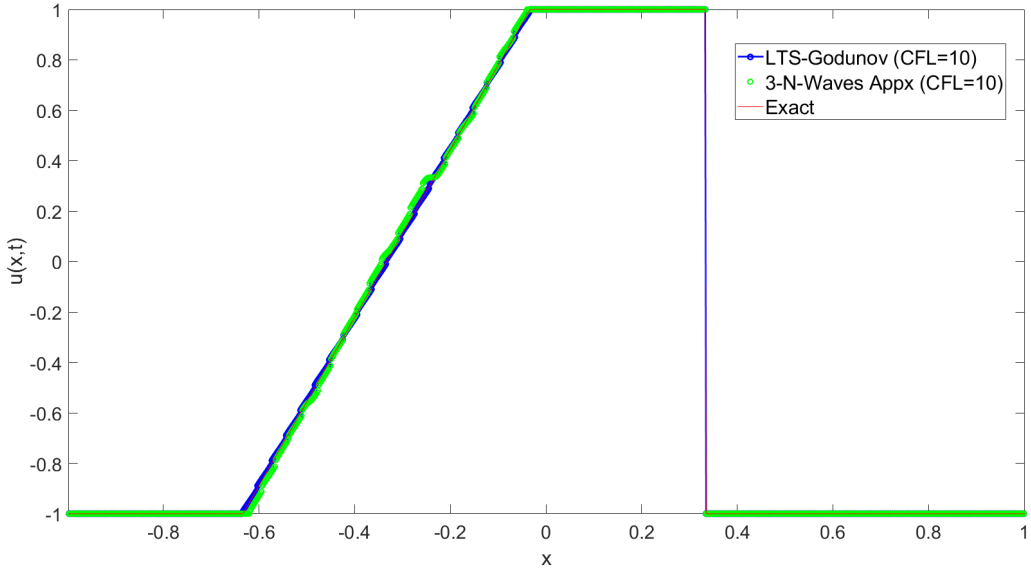

(c) Three-N-waves and LTS-Godunov, CFL=10, N=1000

Figure 4.9: Three-N-waves approximation solution for initial data 4.10

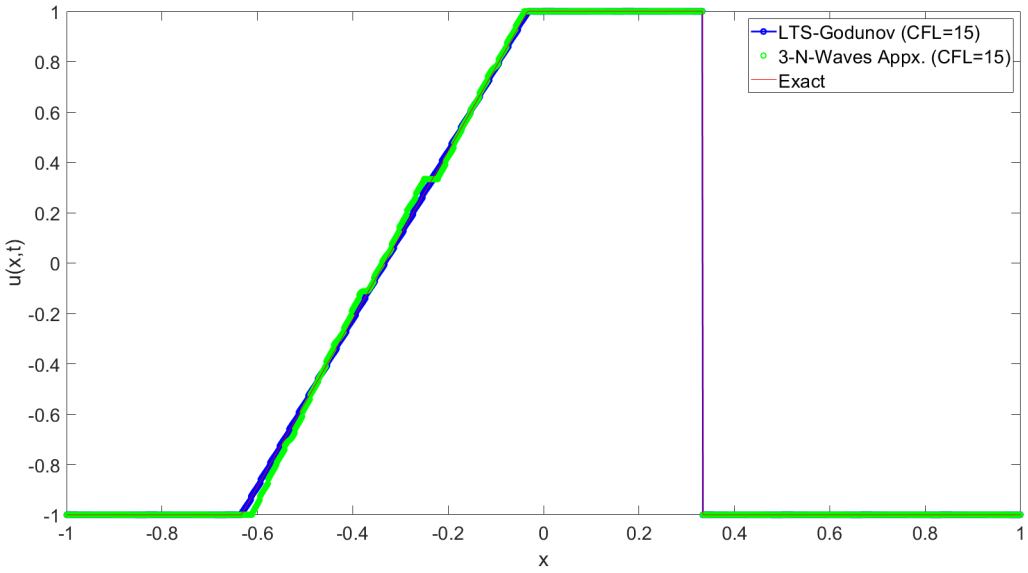

(d) Three-N-waves and LTS-Godunov, CFL=15, N=1500

Figure 4.9: Three-N-waves approximation solution for initial data 4.10 (*cont.*)

4.6 Non-Convex Function (Buckley Leverett)

Since the three-N-waves approximation is an extension and a higher order of accuracy of the two-N-waves approximation, thus the three-N-waves approximation is a good representation and comparing the resolution with the LTS-Godunov scheme. Consider the Buckley-Leverett fractional flow function that was introduced at 3.3 and the initial data with the time domain $t = [0, 0.5]$:

$$u_0(x) = \begin{cases} 0 & , x < 0 \\ \frac{3}{4} & , 0 \leq x \leq 1 \\ 0 & , x > 1 \end{cases} \tag{4.11}$$

where the constant M defined in equation 3.3 is 1 for simplicity. Due to the expensive computational power to numerically solve extrema function ($w(u) = f(u) + iu\frac{\Delta x}{\Delta t}$) in the M function defined in 2.31 for **LTS-Godunov**, where $f(u)$ is the Buckley-Leverett function. The minimum and maximum of $w(u)$ are then solved analytically with a symmetric technique such that:

$$\begin{gathered} w'(u) = 0 \\ \frac{2u(1-u)}{\left(u^2 + (1-u)^2\right)^2} + i\frac{\Delta x}{\Delta t} = 0 \\ \frac{2u(1-u)}{\left(u^2 + (1-u)^2\right)^2} - C = 0 \end{gathered}$$

for

$$u \in D = [0, 1]$$

where

$$C = -i\frac{\Delta x}{\Delta t}$$

Since $f'(u) \geq 0$ for the domain D, thus we can conclude that the equation has no solution for $C < 0$ which also implies that integer i must be more than zero. Using the fact that $f(u)$ is symmetric around $u = \frac{1}{2}$, we make a variable substitution with:

$$u = \frac{1}{2} + a \qquad , a \in \left[-\frac{1}{2}, \frac{1}{2}\right]$$

then $f'(u)$ can be written as

$$\begin{aligned} f'(u) &= \frac{2u(1-u)}{\left(u^2 + (1-u)^2\right)^2} \\ &= \frac{2\left(\frac{1}{2}+a\right)\left(\frac{1}{2}-a\right)}{\left(\left(\frac{1}{2}+a\right)^2 + \left(\frac{1}{2}-a\right)^2\right)^2} \\ &= \frac{2(1-4a^2)}{(1+4a^2)^2} \\ &= \frac{2(1-b)}{(1+b)^2} \end{aligned}$$

where

$$b = 4a^2 = 4\left(u - \frac{1}{2}\right)^2$$

Inserting $f'(u)$ back into the $w'(u)$ function

$$\begin{aligned} \frac{2(1-b)}{(1+b)^2} - C &= 0 \\ Cb^2 + 2(C+1)b + C - 2 &= 0 \end{aligned}$$

Solving quadratically

$$b = \frac{-(C+1) \pm \sqrt{4C+1}}{C}$$

Since b is always positive, thus:

$$b = \frac{-(C+1) + \sqrt{4C+1}}{C}$$

We have defined that

$$u = \frac{1}{2} + a$$

then, $a = \pm\sqrt{\frac{1}{4}b} = \pm\frac{1}{2}\sqrt{b}$

$$\begin{aligned} &= \frac{1}{2} \pm \frac{1}{2}\sqrt{b} \\ &= \frac{1}{2}\left(1 \pm \sqrt{b}\right) \end{aligned}$$

$$u = \frac{1}{2}\left(1 \pm \sqrt{\frac{-(C+1) + \sqrt{4C+1}}{C}}\right)$$

Henceforth, the extreme points of $w(u)$ are of the solved variable u. Thus allowing to compute the minima and maxima in *function* M for the LTS-Godunov scheme. Provided that the constant M is other than 1, there poses increasing complexity in solving analytically, thereby we shall consider constant $M = 1$ in this study. On the other hand, the three-N-waves approximation is solved in accordance with **algorithm 4** outlined in the previous chapter. The solution is shown below with different courant number:

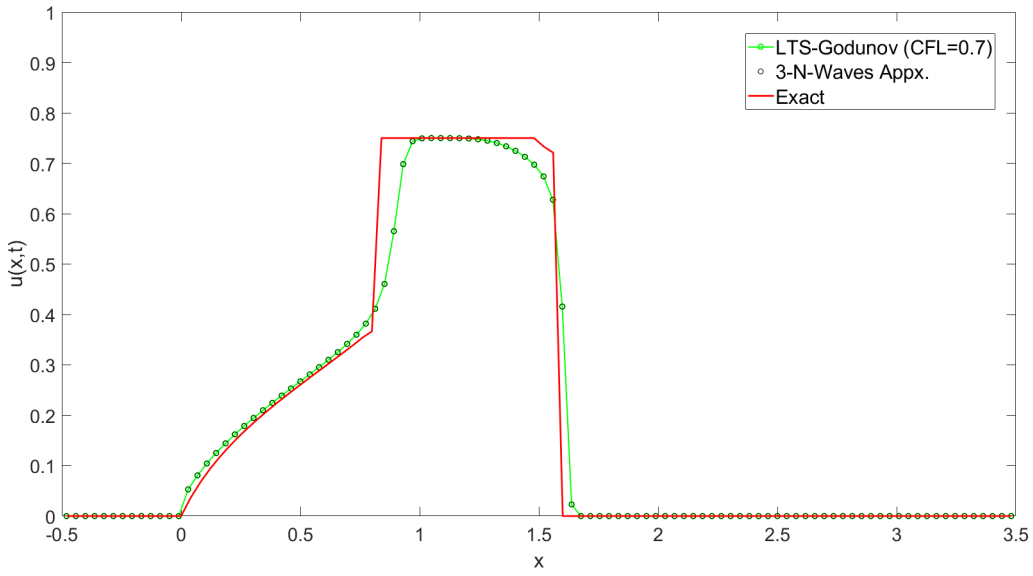

(a) CFL=0.7, N=100

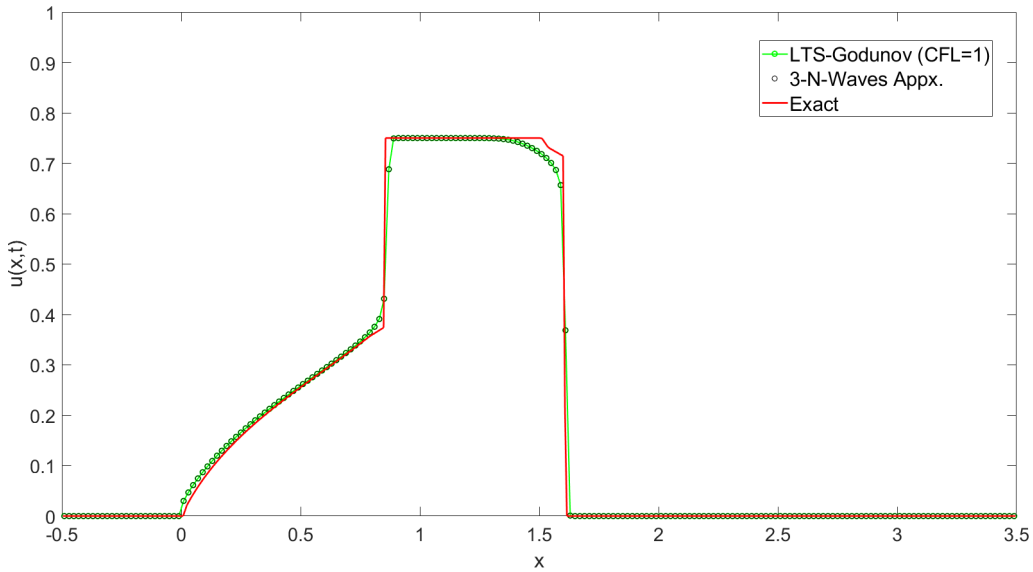

(b) CFL=1, N=200

Figure 4.10: Buckley-Leverett solution for initial data 4.11

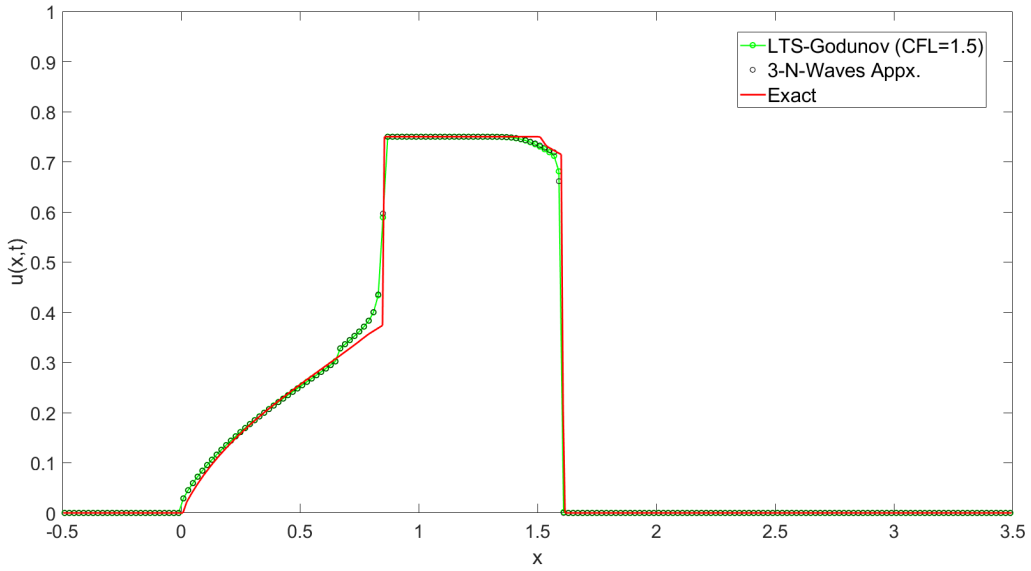

(c) CFL=1.5, N=200

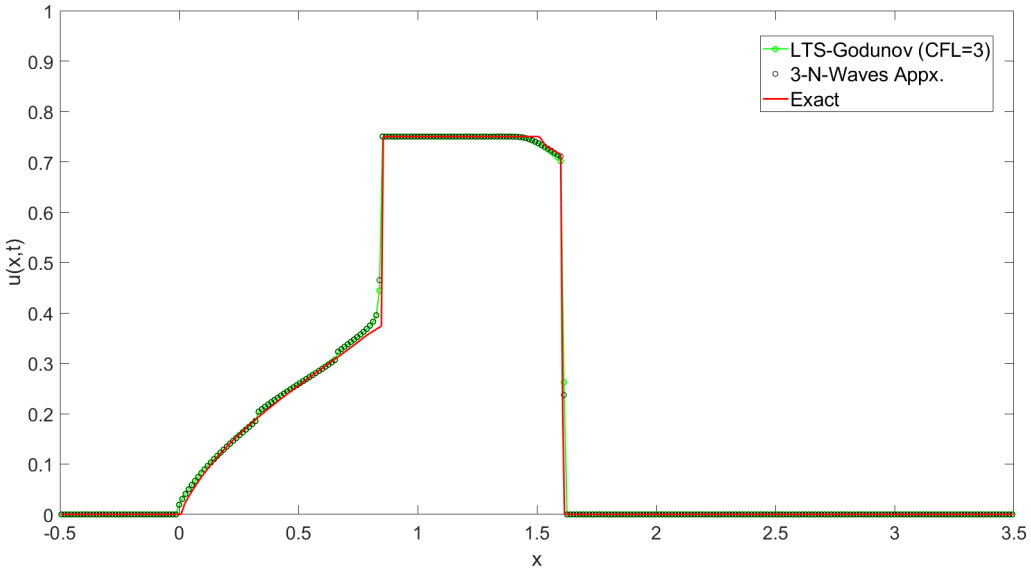

(d) CFL=3, N=300

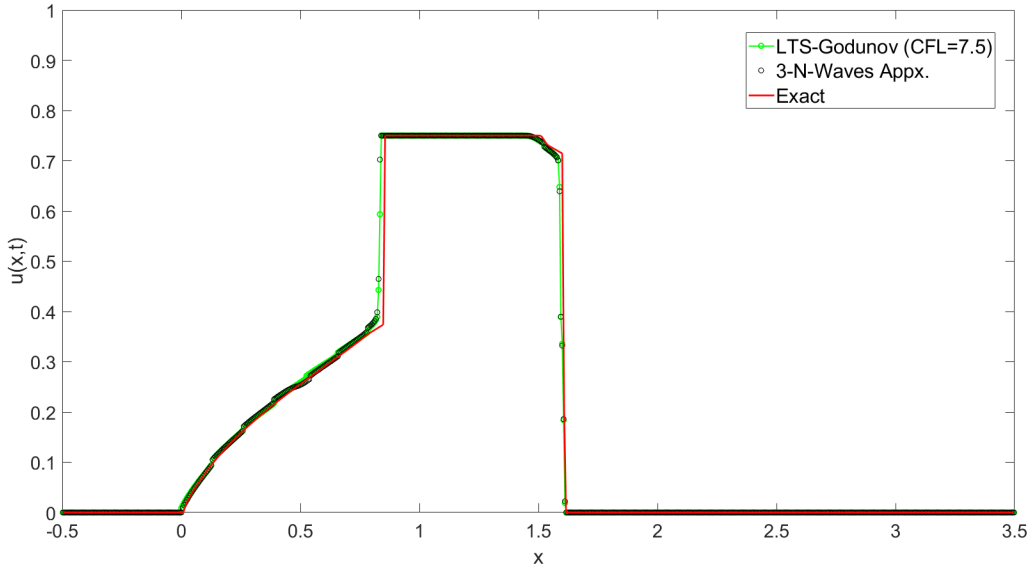

(e) CFL=7.5, N=700

Figure 4.10: Buckley-Leverett solution for initial data 4.11 (*cont.*)

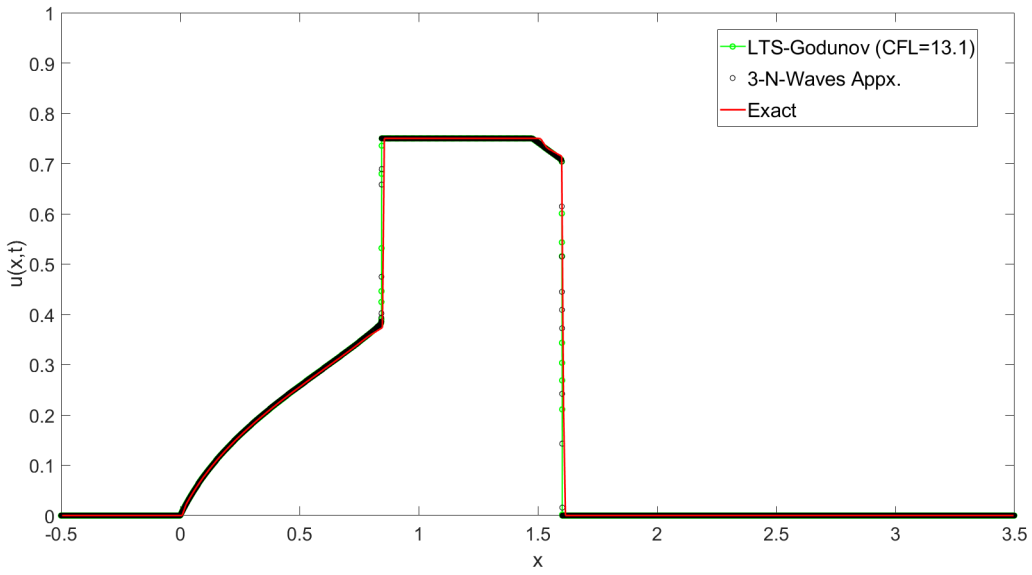

(f) CFL=13.1, N=15000

Figure 4.10: Buckley-Leverett solution for initial data 4.11 (*cont.*)

The increasing jump initially at $x = 0$ is transformed into a rarefaction wave followed by a shockwave, while the decreasing jump at $x = 1$ comprises a brief rarefaction wave followed by a jump. We see that when CFL=0.7, LTS-Godunov and three-N-waves scheme struggles to solve the first shockwave from the left followed by the rarefaction wave. When CFL increases to 1, both schemes have that shockwave to be resolved with smoother lines, while it shows no clear indication of improvement for the curve corresponding to the small rarefaction wave between two shockwaves. As the solution gradually advances to the LTS-schemes that is CFL>1, LTS-Godunov displays an increasingly smoother rarefaction wave solution between the two shocks. Similarly, with the increase of grid cells, the three-N-wave approximation presents the behaviour of approaching to the exact solution on par with the LTS-Godunov scheme.

Chapter 5

Conclusion

We have shown that the large time step scheme particularly Godunov and Roe for hyperbolic conservation law as the underlying foundations for solving the non-convex problem. Furthermore, the wave addition scheme is refashioned to two/three-N-waves approximation and was compared to LTS schemes, it was investigated theoretically to enable both methods to be comprehended with better cohesion, then numerical experiments are conducted in order to validate the premises.

5.1 Large Time Step Scheme

We have presented several methods to solving conservative schemes such as Roe, Lax-Friedrichs, Lax-Wendroff and Godunov that lays as the cornerstone for large time step schemes. Then, schemes such as Godunov, LTS-Roe are presented in numerical experiments to solidify the foundations for further investigation. A breakthrough which was to solve system of equations with LTS schemes specifically LTS-Roe. Followed by replication of tests 1 and 2 in Dong's paper. Instead of reproducing it with LTS-WA in the paper, it was presented with LTS-Roe and LTS-Godunov to compare the results. At which LTS-Roe is the equivalence of LTS-WA when solving linear equations. Furthermore, LTS-Roe is interpreted as the "one-N-wave approximation" due to its linearity. In test 2 for Burger's equation, LTS-Godunov is used as the similitude for LTS-WA. The results are identical to Dong's paper, further consolidate the wave-addition scheme is an alternate interpretation of the LTS-Godunov scheme when the function transcends linear equation.

5.2 Two/Three-N-waves Approximation

The original 'two-waves appx.' and 'three-waves appx.' are reformulated with a more extensive and general algorithm in handling all kinds of functions, relabelling it as 'two-N-waves appx.' and 'three-N-waves appx.'. With regards to reproducing the second part of test 2 in Dong's paper that is test 3 in this thesis, despite there is an ambiguity of the number of grid cells used in Dong's paper, the three-waves approximation results generated are still closely resembling each other. And more importantly, with the increase in the number of grid cells and larger courant number, the more 'seamless' the result in a way that more discontinuities are introduced rendering inconspicuous jumps at the rarefaction wave.

The major goal that is to investigate LTS schemes and three-N-waves approximation on the non-convex function are presented in section 4.6. The findings are that LTS-Godunov and three-N-wave approximation display near-identical plots. At CFL ≤ 1, the solution fails to resolve the second rarefaction. And as CFL increases, the rarefaction wave improves greatly in which the curve at second rarefaction is more prominent and congruent to the exact or analytical solution.

Conclusively, LTS-Godunov and N-waves approximation schemes are proven to be numerically stable in solving hyperbolic conservation law for a non-convex function.

5.3 Recommendation

While saving the computational time to determine the extrema of the extrema function $(f(u) + iu\frac{\Delta x}{\Delta t})$, an analytical solution was devised, however, it was only limited to constant M in Buckley-Leverett function to be 1. Therefore, further study shall be considered in solving the extrema function with constant M analytically other than 1.

Bibliography

[1] Haitao Dong and Fujun Liu. "Large time step wave adding scheme for systems of hyperbolic conservation laws". In: *Journal of Computational Physics* 374 (2018), pp. 331–360.

[2] Guang-Shan Jiang and Chi-Wang Shu. "Efficient implementation of weighted ENO schemes". In: *Journal of computational physics* 126.1 (1996), pp. 202–228.

[3] Randall J LeVeque. "A large time step generalization of Godunov's method for systems of conservation laws". In: *SIAM journal on numerical analysis* 22.6 (1985), pp. 1051–1073.

[4] Randall J LeVeque. "Convergence of a large time step generalization of Godunov's method for conservation laws". In: *Communications on pure and applied mathematics* 37.4 (1984), pp. 463–477.

[5] Randall J LeVeque and Randall J Leveque. *Numerical methods for conservation laws*. Vol. 132. Springer, 1992.

[6] Sofia Lindqvist et al. "Large time step TVD schemes for hyperbolic conservation laws". In: *SIAM Journal on Numerical Analysis* 54.5 (2016), pp. 2775–2798.

[7] Rolf Nygaard. "Large Time Step Methods for Hyperbolic Partial Differential Equations". MA thesis. NTNU, 2017.

[8] Marin Prebeg. "Large Time Step Methods for Hyperbolic Conservation Laws". In: (2017).

[9] ZhanSen Qian and Chun-Hian Lee. "A class of large time step Godunov schemes for hyperbolic conservation laws and applications". In: *Journal of Computational Physics* 230.19 (2011), pp. 7418–7440.

Appendices

Appendix A (Dong's Test 1 Figure 9 [1])

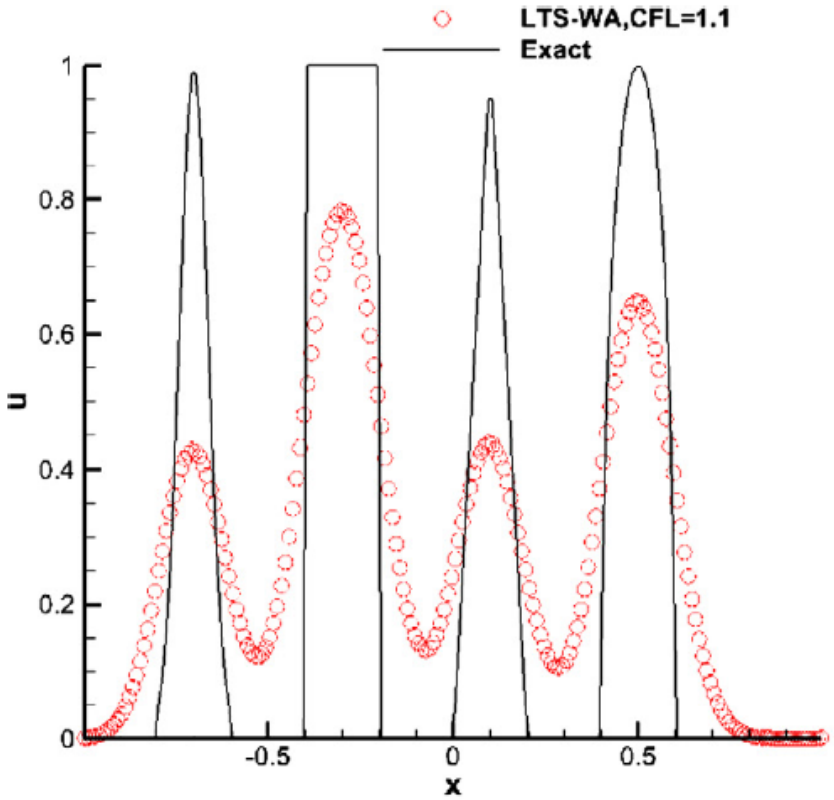

(a) LTS-WA, CFL=1.1, N=200

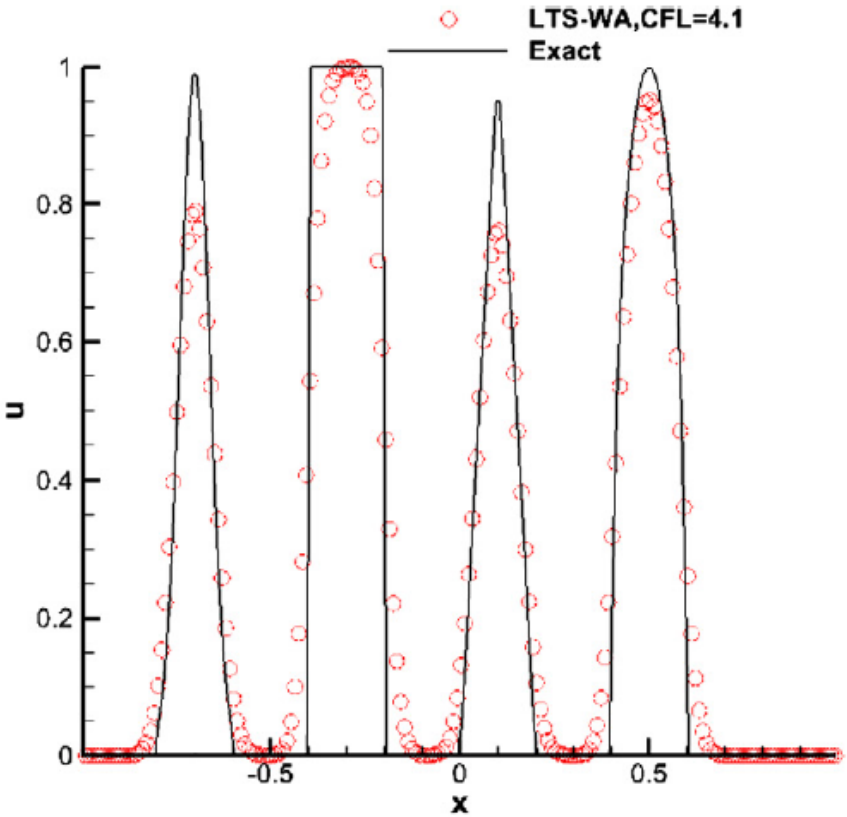

(b) LTS-WA, CFL=4.1, N=400

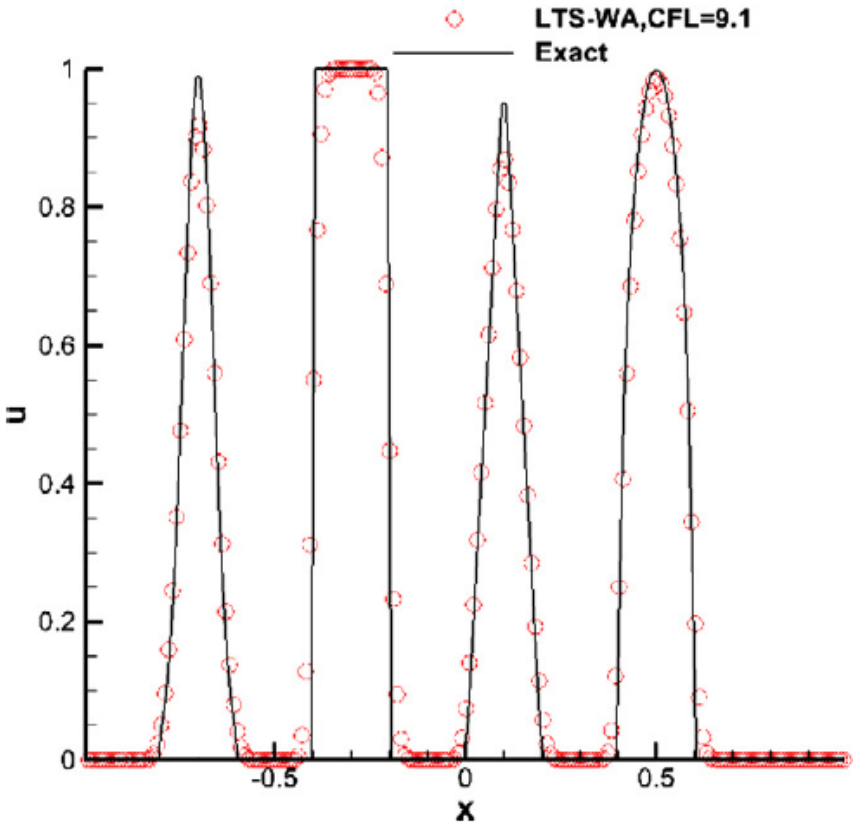

(c) LTS-WA, CFL=9.1, N=600

Appendix B (Dong's Test 2 Figure 10 [1])

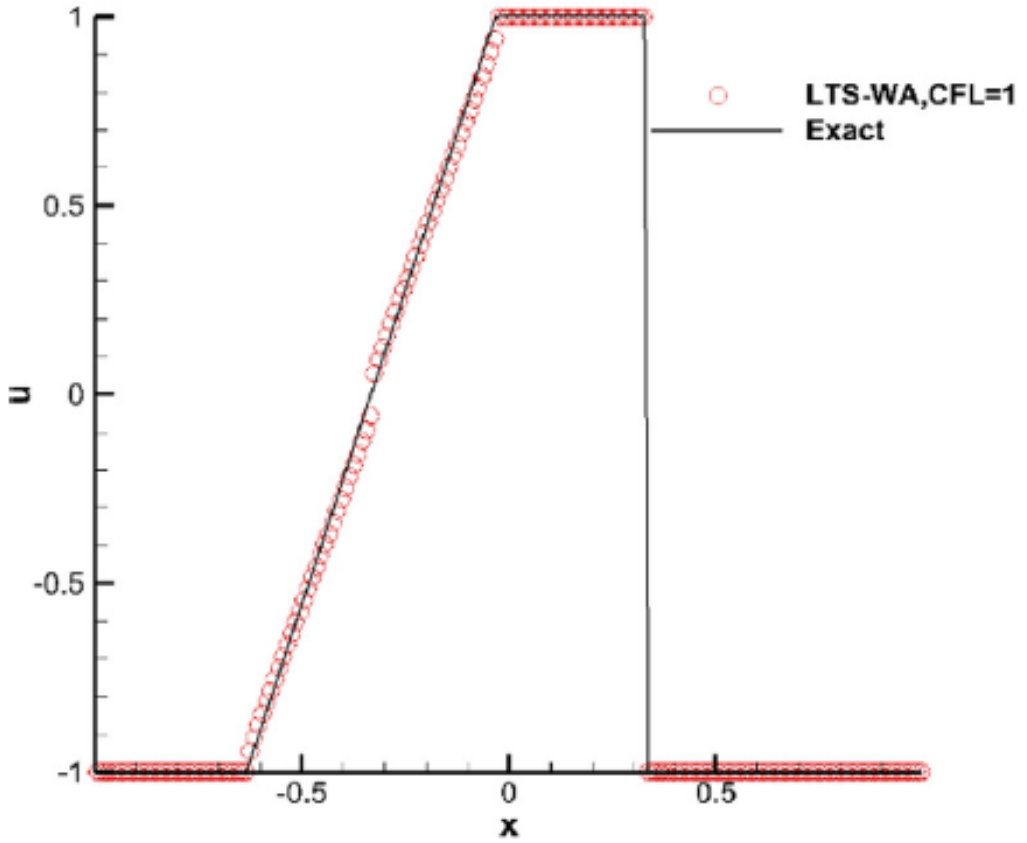

(a) LTS-WA, CFL=1, N=200

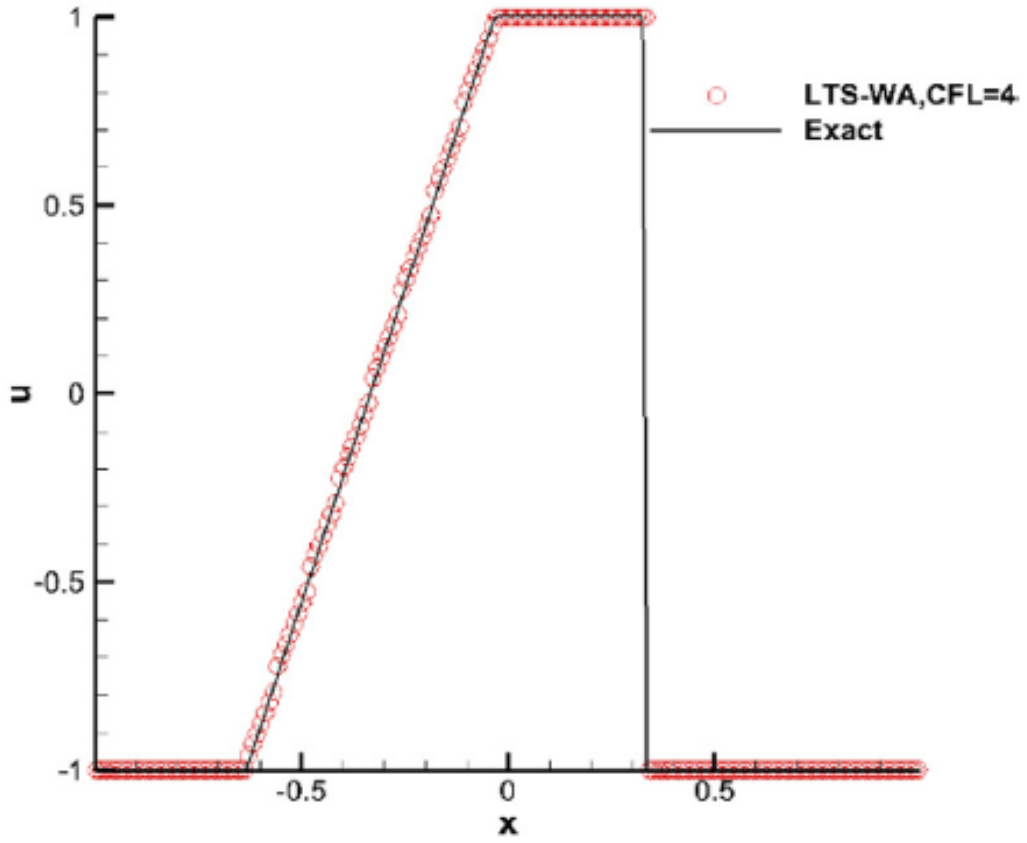

(b) LTS-WA, CFL=4, N=400

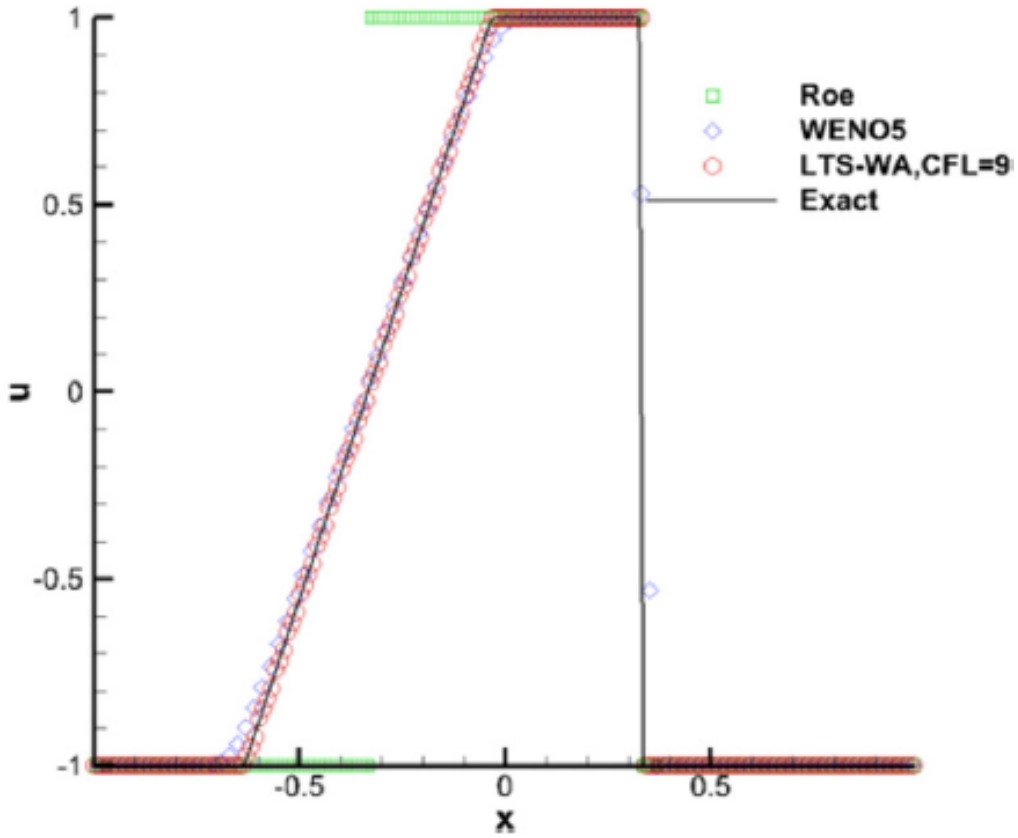

(c) LTS-Roe, WENO5 and LTS-WA, CFL=9, N=600

Appendix C (Dong's Test 2 Figure 11 [1])

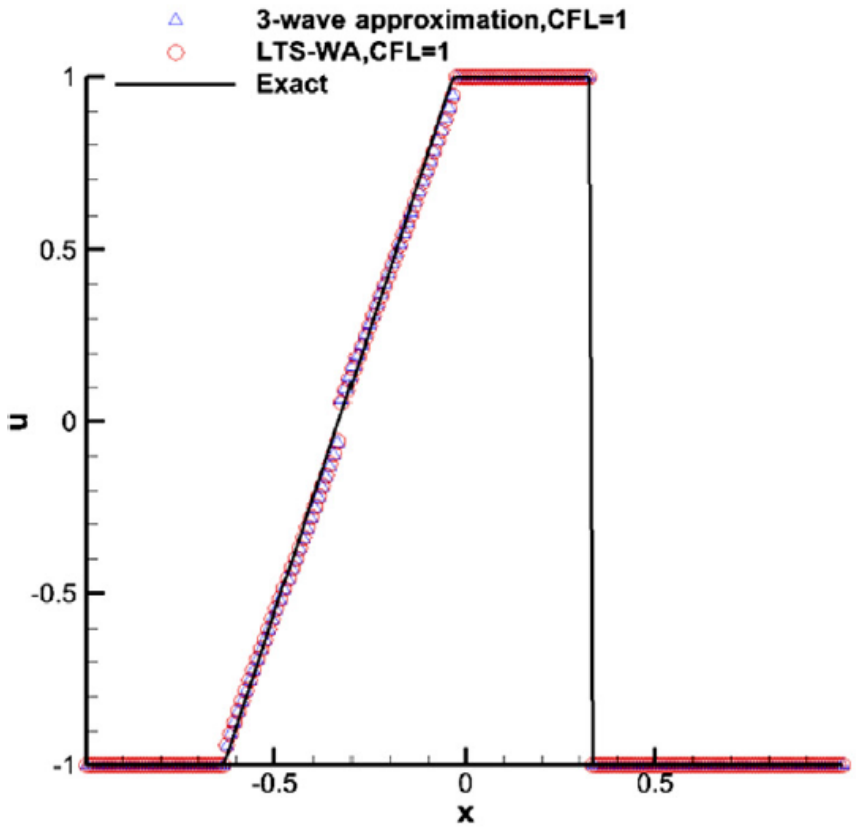

(a) 3-wave appx. and LTS-WA, CFL=1

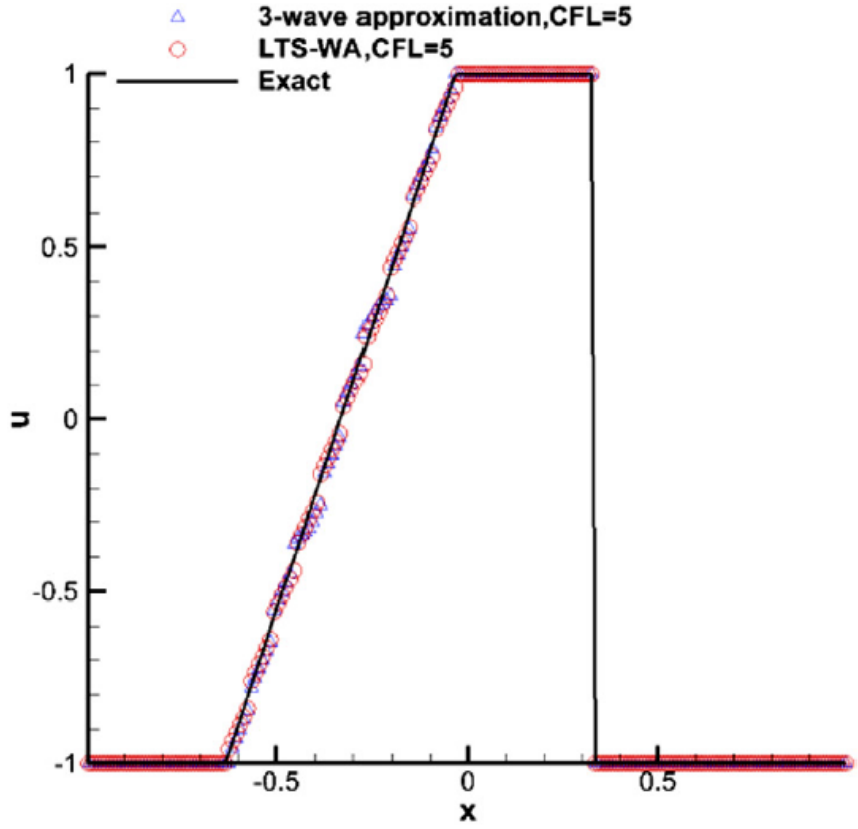

(b) 3-wave appx. and LTS-WA, CFL=5

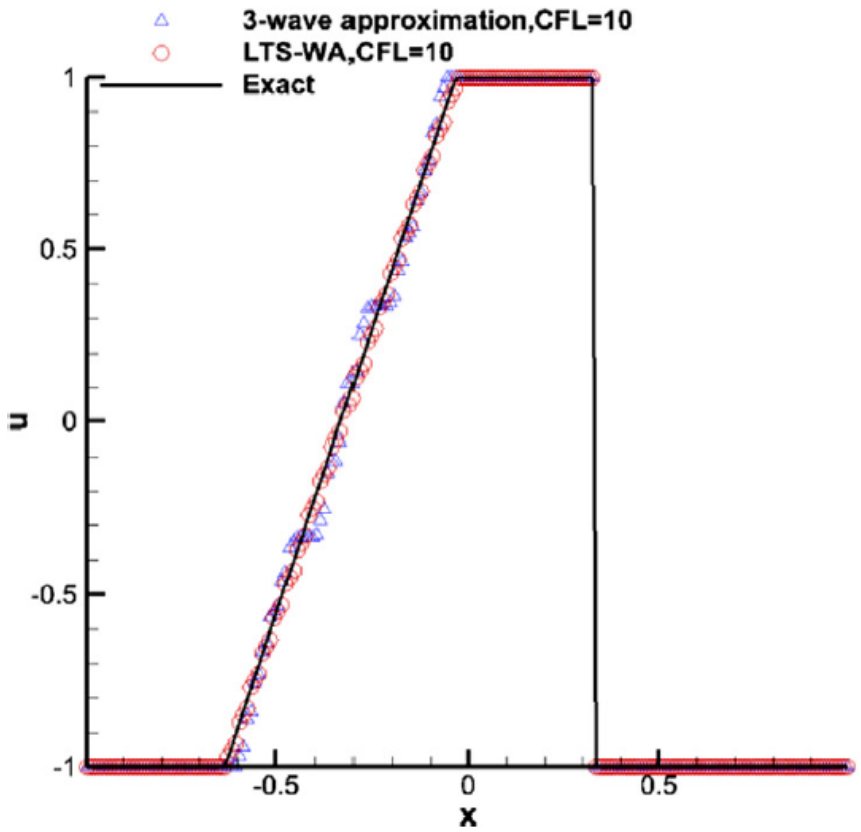

(c) 3-wave appx. and LTS-WA, CFL=10

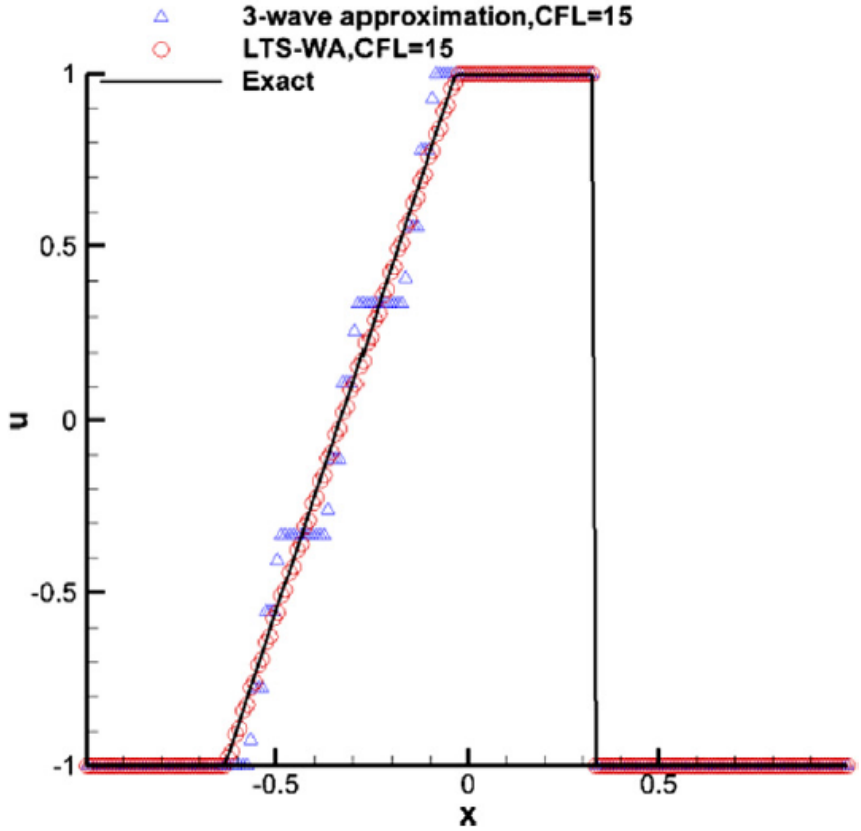

(d) 3-wave appx. and LTS-WA, CFL=15